MDPI

Article

Dynamics for a Nonlinear Stochastic Cholera Epidemic Model under Lévy Noise

Qura Tul Ain [1], Anwarud Din [2], Xiaoli Qiang [3] and Zheng Kou [1,*]

1   Institute of Computing Science and Technology, Guangzhou University, Guangzhou 510006, China; quratulain@gzhu.edu.cn
2   Department of Mathematics, Sun Yat-Sen University, Guangzhou 510275, China; anwarud@mail.sysu.edu.cn
3   School of Computer Science and Cyber Engineering, Guangzhou University, Guangzhou 510006, China; qiangxl@gzhu.edu.cn
*   Correspondence: kouzheng@gzhu.edu.cn

Abstract: In this study, we develop a comprehensive mathematical model to analyze the dynamics of epidemic cholera, characterized by acute diarrhea due to pathogen overabundance in the human body. The model is first developed from a deterministic point of view, and then it is modified to include the randomness by stochastic differential equations. The study selected Lévy noise above other well-known types of noise, emphasizing its importance in epidemic modeling. Besides presenting a biological justification for the stochastic system, we demonstrate that the equivalent deterministic model exhibits possible equilibria. The introduction is followed by theoretical analysis of the model. Through rigorous analysis, we establish that the stochastic model ensures a unique global solution. Lyapunov function theory is applied to construct necessary conditions, which on average, guarantee the model's stability for $\mathbb{R}_0^s > 1$. Our findings suggest the likelihood of eradicating the disease when $\mathbb{R}^s$ is below one, a significant insight supported by graphical simulations of the model. Graphical illustrations were generated from simulating the model in order to increase the analytical results' robustness. This work provides a strong theoretical framework for a thorough comprehension of a range of such diseases. This research not only provides a deeper understanding of cholera dynamics but also offers a robust theoretical framework applicable to a range of similar diseases, alongside a novel approach for constructing Lyapunov functions for nonlinear models with random disturbances.

Keywords: Lévy noise; threshold; extinction; persistence; numerical simulation

MSC: 15B51; 26A18; 37H05

1. Introduction

Vibrio cholera is a pathogen that causes cholera and is mostly found in marine animals, and this disease is characterized by intestinal infections. There are over 200 known serogroups in this bacterium species, which spans a wide variety. Nevertheless, among these serogroups, only O139 and O1 can cause cholera illnesses [1,2]. Surprisingly, these bacteria have an amazing ability to withstand the harsh acidic environment of the stomach before they rupture the mucous membrane that covers the epithelial cells of the intestine [1,3]. The colonized gut produces enterotoxins, which cause the small intestine's endothelial cells to secrete more water and electrolytes in response [1]. In 1854, John Snow demonstrated that consuming contaminated food or water might potentially trigger cholera outbreaks [4]. There are, nonetheless, other channels of transmission. For instance, the virus may spread among those who are susceptible through contact with ill persons. These individuals may spread the disease to other family members who cook or share water containers if they are more likely to get it [4]. People can spread the virus even if they do not show any symptoms, and symptoms can appear anywhere from a few hours to five days following infection. Still, symptoms usually start to appear in the first two to three

days [5]. Watery diarrhea, vomiting, and severe leg cramps are common symptoms of the condition. Patients who have an infection must receive treatment as soon as possible, since waiting too long increases the danger of dehydration, acidosis, and circulatory collapse. Notably, there is a 12 to 24 h mortality risk associated with severe episodes of this condition [4,6]. Studies indicate that those who make a full recovery can become immune to the disease for a duration of 3 to 10 years. However, studies also indicate that this immunity may diminish a few weeks or months afterward [4,7]. Due in part to the challenges associated with obtaining clean water and sanitary facilities in developing and underdeveloped countries, diarrheal illnesses continue to be the leading cause of death for newborns and young children [8]. Moreover, as noted by Sun et al. [9], this disease has a poor surveillance system and poses a serious risk to human civilization because of its high rates of morbidity and mortality. Therefore, to comprehend the disease's progression and develop control measures, it is imperative to look at mathematical models that make clear the paths by which cholera is transmitted.

The literature, including references [1,4,6–9], has evaluated some mathematical models to understand the cholera transmission patterns. Two different bacterial concentrations—less-infectious and antibiotic-resistant—were included in the work reported in [7] to create the Susceptible–Infectious–Recovered (SIR) model. Within the infected category, asymptomatic and symptomatic subcategories were further differentiated. The authors investigated the cost-effectiveness of several management strategies in two communities that were assumed to have endemic cholera through the use of numerical simulations, optimal control theory, and sensitivity analysis. Furthermore, the SIR-type model that Wang and Modnak [10] studied included a class that deals with vibrio bacterium abundance in the environment. The strategy includes three preventative measures: vaccines, clean water, and medical treatment. The authors determined the stability of the equilibrium points by assigning constant values to the control parameters. Using Pontryagin's Maximum Principle, they carried out a further examination of a more comprehensive cholera model with time-dependent controls. This study demonstrated the optimum control problem's solution and provided the required optimality conditions. The authors in [6] incorporated a variety of control strategies, including treatment, immunization, isolation, and public health awareness campaigns. In addition, the model had a separate class for the microbe concentration. By comparing the combined threshold parameter and the basic reproduction number with threshold values linked to therapy, immunization, and education, the authors carried out a comparison study. The purpose of this study was to examine possible advantages for the community. The authors used a Lyapunov functional technique to examine the stability of fixed points.

As highlighted in references [11–18], the use of mathematical modeling tools is highly advised for examining the dynamics of epidemic spread and developing successful control strategies. These models provide a well-rounded approach by bridging the gap between biological scenario to show the infection's natural progression and its dependency on the associated data. Many researchers developing models that shed light on cholera dynamics-related topics. Reference [19] highlights the great interest of epidemiologists researching the dynamics and management of cholera epidemics in including environmental factors for a more thorough understanding, even though most models use a deterministic approach. Unpredictable factors, such as social interactions or other population features, such the onset and spread of diseases, worsen the situation. That being said, the diversity and unpredictable nature of an epidemic's environment can have a substantial impact on both its current and future behavior.

Stressing the critical connection between bacterial persistence and spread and environmental changes is essential. The dynamics of an infection necessarily involve stochastic components, impacting both parameters and states. In epidemic modeling, stochasticity is acknowledged by epidemiology as a basic component. The model's disturbances are random by nature, but they also have to show positive autocorrelation. Moreover, these variations may be obtained analytically from the related issue by using the probability

density function, as is covered in references [20–22]. The two main methods used in epidemic modelling are stochastic and deterministic. The stochastic modelling technique is frequently preferred in biological system modelling because it can provide a more realistic model than deterministic models, as sources [23–26] emphasize. Determining a distribution of expected outcomes, such as the number of infected people over time, *t*, is made easier using stochastic differential equations (SDEs). Furthermore, a stochastic model creates various outcomes through repeated simulations, delivering more meaningful information than deterministic models.

To better understand the dynamics of cholera transmission and its long-term behavior in the setting of moving populations that are prone to bacterial contamination, we built a stochastic epidemic model in the current study. Both people and microbes are included in the population, which is divided into four compartments. The susceptible, infected, recovered, and pathogen groups are represented by the compartments with the designations $\mathcal{S}(t)$, $\mathcal{I}(t)$, $\mathcal{R}(t)$, and $\mathcal{B}(t)$, respectively. Lévy noise is crucial in modeling systems where significant, abrupt changes are important. It captures both continuous fluctuations and discrete jumps, making it essential for realistic dynamics in various phenomena. In the context of epidemic modeling, such as in SIR models, Lévy noise allows us to simulate sudden large-scale changes like super-spreading events that are not well modeled by Gaussian noise alone.

Lévy noise derives from Lévy processes, which extend Brownian motion to include jumps, providing a more comprehensive representation of random phenomena. These processes have independent, stationary increments and stochastically continuous paths, ideal for modeling sudden, unpredictable changes in dynamic system.

The characteristic function of a Lévy process is given by [27],

$$\mathbb{E}[e^{iuL(t)}] = \exp\left(t\left(iu\gamma - \frac{1}{2}\sigma^2 u^2 + \int_{\mathbb{R}\setminus\{0\}} (e^{iux} - 1 - iux\mathbf{1}_{|x|<1})\nu(dx) \right) \right),$$

where γ represents the drift coefficient, σ^2 is the variance of the Gaussian part, and ν is the Lévy measure that describes the jump intensity and distribution. This formulation enables the modeling of both minor fluctuations and major shifts within a single framework. In stochastic SIR models, incorporating Lévy noise enhances the model's ability to reflect the inherent variability and unpredictability of epidemic spread. It is particularly effective in accounting for overdispersion in disease transmission rates, which is a common real-world phenomenon [28,29].

Lévy noise is included in the model as it has more benefits over normal Gaussian noises, particularly in disease-related mathematical models. More specifically, we take into account the period between getting the infection and the moment at which symptoms appear in a person.

1.1. Motivation

The impetus for this research is the critical challenge posed by cholera, a global public health concern. Current deterministic models serve as a foundation but are limited in their ability to represent the stochastic behaviors and intricate patterns of disease transmission. Given the direct impact of environmental factors on cholera's spread, there is a clear necessity for a model that incorporates stochasticity to reflect the unforeseen fluctuations and perturbations that characterize epidemic outbreaks.

The motivation for integrating Lévy noise into our epidemic modeling framework stems from its proven ability to capture the inherently random and discontinuous nature of disease transmission, which traditional Gaussian noise models often fail to represent accurately. Recognized for its capacity to model random fluctuations with unpredictable jumps, Lévy noise provides a more realistic simulation of the stochastic dynamics observed in real-world disease outbreaks. This approach is particularly relevant for diseases like cholera, where transmission through multiple vectors introduces additional complexity and unpredictability. Studies [30–32] have demonstrated that Lévy noise can significantly

reduce the disease extinction threshold and enhance the suppression of outbreaks in network-based models, making it a compelling choice for our analysis. Further support for the use of Lévy noise is provided by [31], who found that it could influence the dynamics of hepatitis B more effectively than Gaussian noise, highlighting its potential in enhancing disease modeling across various epidemiological contexts [31]. These findings collectively motivate our choice of Lévy noise to achieve a deeper understanding of the transmission dynamics and control strategies for cholera, aiming to provide insights that are not only theoretically rigorous but also practically applicable in public health responses.

1.2. Contribution

This paper endeavors to contribute to the field of epidemic modeling by introducing a novel approach to understanding cholera dynamics. The primary contributions are twofold. First, we propose a mathematical model that extends the conventional Susceptible–Infectious–Recovered (SIR) framework. Our model incorporates the pathogen concentration explicitly, aiming to provide a more nuanced view of the transmission mechanisms of cholera.

Second, we integrate Lévy noise into the epidemic model. This integration seeks to capture the unpredictable fluctuations in disease spread more accurately than traditional deterministic models. Specifically, the Lévy noise is adept at modeling sudden and sporadic changes, which are characteristic of real-world disease dynamics. This enhancement allows our model to better reflect the complex interplay between environmental variables and human behavior that influences cholera propagation.

Through the analysis of this stochastic model, we uncover insights into the thresholds that govern disease persistence versus extinction. These findings have potential implications for public health strategies. Additionally, we introduce a novel technique for constructing Lyapunov functions, which facilitates the examination of stationary distributions in nonlinear systems affected by random perturbations. Although demonstrated in the context of cholera, this method has the potential for application to a variety of infectious diseases.

2. Models Formulation

In this section, we proposed a mathematical model employing the spread of cholera disease with environmental exposure. Thus, we will build a model that integrates the Susceptible–Infectious–Recovered ($\mathcal{SIR}$) framework and takes into consideration the pathogen's concentration or population density while describing the dynamics of cholera. The whole human population $\mathsf{N}(t)$ is divided into three sub-groups at every given time $t \geq 0$: susceptible $\mathcal{S}(t)$, infected $\mathcal{I}(t)$, and recovered $\mathcal{R}(t)$. The sizes of people in each category are represented by the respective sub-groups. Moreover, $\mathcal{B}(t)$ represents the amount of bacteria present in the food or water. The letter ξ refers to the continuous influx that the population experiences. We add a uniform mortality rate $\mu > 0$, which applies evenly across all compartments. Two types of interactions were assumed: β_1 represents the interaction between the human population and the environment and β_2 represents the interaction between humans. The notion γ is the recovery rate of the infected individuals and η is the inflow rate of cholera bacteria from the infected human. The vibratory bacteria are perishing at a steady δ pace. In addition to this, we have enforced the further supposition onto the model:

A_1 : Every parameter within the system is a non-negative, positive real number.

A_2 : Both the pathogen in the environment and every individual in the population have the same probability of shifting into a new class. Put another way, the movement probability between the compartments is determined by the distribution of exponential types. The inverse of that parameter in an exponential distribution may be used to calculate the estimated average time spent in a class.

A_3 : We assume a constant population in a sense that no infection can enter into the community neither we assume immigration into the population, and the only inflow

into the susceptible compartment is due to births. This implies that the disease is solely spreading inside the population and that external infections have no effect on the dynamics of the epidemic.

A_4 : Individuals who have recovered from cholera are no longer vulnerable to the disease and so do not need medical care. People who have recovered from cholera cannot exit the group and natural death is the sole way for a cholera-recovered individual to leave the class.

The resulting mathematical model from the previously stated assumptions is as follows:

$$
\begin{aligned}
\frac{\mathcal{S}(t)}{dt} &= \xi - \frac{\beta_1 \mathcal{B}(t)\mathcal{S}(t)}{\mathsf{N}(t)} - \frac{\beta_2 \mathcal{I}(t)\mathcal{S}(t)}{\mathsf{N}(t)} - \mu \mathcal{S}(t), \\
\frac{\mathcal{I}(t)}{dt} &= \frac{\beta_1 \mathcal{B}(t)\mathcal{S}(t)}{\mathsf{N}(t)} + \frac{\beta_2 \mathcal{I}(t)\mathcal{S}(t)}{\mathsf{N}(t)} - (\mu + \gamma)\mathcal{I}(t), \\
\frac{\mathcal{R}(t)}{dt} &= \gamma I(t) - \mu \mathcal{R}(t), \\
\frac{\mathcal{B}(t)}{dt} &= \eta \mathcal{I}(t) - \delta \mathcal{B}(t).
\end{aligned}
\tag{1}
$$

The state transition diagram of the proposed $\mathcal{SIRB}$ model is demonstrated in Figure 1.
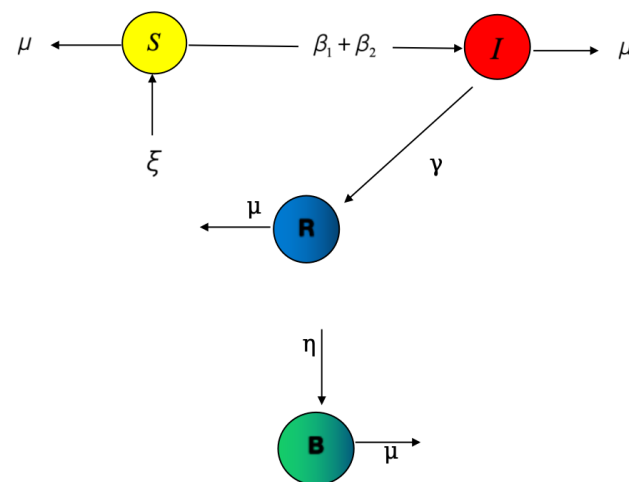
Figure 1. Flow chart of the proposed model (1).

Fundamental Properties of Model (1)

Proposition 1. *For the system of differential equations given above, under the Lipschitz condition and continuity in the variable t, there exists a unique solution* $(\mathcal{S}(t), \mathcal{I}(t), \mathcal{R}(t), \mathcal{B}(t))$ *for each initial condition* $(\mathcal{S}(0), \mathcal{I}(0), \mathcal{R}(0), \mathcal{B}(0))$, *which continues to exist for all* $t \geq 0$.

Proof. Define the vector

$$
\mathbf{X}(t) = \begin{bmatrix} \mathcal{S}(t) \\ \mathcal{I}(t) \\ \mathcal{R}(t) \\ \mathcal{B}(t) \end{bmatrix},
$$

and

$$\mathbf{f}(\mathbf{X}(t),t) = \begin{bmatrix} \xi - \frac{\beta_1 \mathcal{B}(t)\mathcal{S}(t)}{\mathsf{N}(t)} - \frac{\beta_2 \mathcal{I}(t)\mathcal{S}(t)}{\mathsf{N}(t)} - \mu \mathcal{S}(t) \\ \frac{\beta_1 \mathcal{B}(t)\mathcal{S}(t)}{\mathsf{N}(t)} + \frac{\beta_2 \mathcal{I}(t)\mathcal{S}(t)}{\mathsf{N}(t)} - (\mu + \gamma)\mathcal{I}(t) \\ \gamma \mathcal{I}(t) - \mu \mathcal{R}(t) \\ \eta \mathcal{I}(t) - \delta \mathcal{B}(t) \end{bmatrix}.$$

Each component of $\mathbf{f}(\mathbf{X}(t),t)$ is a polynomial in terms of $\mathcal{S}, \mathcal{I}, \mathcal{R}, \mathcal{B}$.

Since polynomials are continuously differentiable [33,34], $\mathbf{f}(\mathbf{X}(t),t)$ is Lipschitz continuous in $\mathbf{X}$ on any compact subset of $\mathbb{R}^4$. Therefore, by the Lipschitz condition, there exists a constant $L > 0$ such that for any $\mathbf{X}, \mathbf{Y} \in \mathbb{R}^4$, the inequality $\|\mathbf{f}(\mathbf{X},t) - \mathbf{f}(\mathbf{Y},t)\| \le L\|\mathbf{X} - \mathbf{Y}\|$ holds for all t [35].

By the Picard–Lindelöf theorem [36], given the Lipschitz continuity of $\mathbf{f}$ and the initial condition $\mathbf{X}(0) = \begin{bmatrix} \mathcal{S}(0) \\ \mathcal{I}(0) \\ \mathcal{R}(0) \\ \mathcal{B}(0) \end{bmatrix}$, there exists a unique solution $\mathbf{X}(t)$ that satisfies this system of ODEs for all $t \ge 0$. □

This proof confirms that the deterministic part of our model behaves predictably under these conditions, which allows us to introduce stochastic elements as perturbations to this deterministic framework, contributing to a deeper understanding of the system's behavior under uncertainty.

Proposition 2. *Given the non-negative initial conditions $\mathcal{S}(0), \mathcal{I}(0), \mathcal{R}(0), \mathcal{B}(0)$ and positive parameters $\xi, \mu, \beta_1, \beta_2, \gamma, \eta, \delta$, the solutions $\mathcal{S}(t), \mathcal{I}(t), \mathcal{R}(t), \mathcal{B}(t)$ of the system are bounded for all $t \ge 0$.*

Proof. Summing all four equations of model, we obtain

$$\frac{d}{dt}(\mathcal{S}(t) + \mathcal{I}(t) + \mathcal{R}(t) + \mathcal{B}(t)) = \xi - \mu(\mathcal{S}(t) + \mathcal{I}(t) + \mathcal{R}(t) + \mathcal{B}(t)).$$

Let $\mathsf{N}(t) = \mathcal{S}(t) + \mathcal{I}(t) + \mathcal{R}(t) + \mathcal{B}(t)$. The equation simplifies to

$$\frac{d\mathsf{N}(t)}{dt} = \xi - \mu \mathsf{N}(t).$$

This is a linear first-order ordinary differential equation, which can be solved using an integrating factor

$$N(t) = \frac{\xi}{\mu} + \left(N(0) - \frac{\xi}{\mu}\right)e^{-\mu t}.$$

As $t \to \infty$, $\mathsf{N}(t) \to \frac{\xi}{\mu}$. Therefore, $\mathsf{N}(t)$ is bounded by $\frac{\xi}{\mu}$ for all $t \ge 0$, assuming $N(0)$ is finite.

Since $\mathcal{S}(t), \mathcal{I}(t), \mathcal{R}(t)$, and $\mathcal{B}(t)$ are all non-negative and part of $\mathsf{N}(t)$, they are individually bounded as well. Specifically, each of these variables is bounded by $\frac{\xi}{\mu}$, as none can exceed $\mathsf{N}(t)$.

This completes the proof that the solutions $\mathcal{S}(t), \mathcal{I}(t), \mathcal{R}(t)$, and $\mathcal{B}(t)$ to the system are bounded, ensuring the model's stability over time. □

Through some basic mathematical computations, we can easily derive the disease-free equilibrium (DFE) points for the model outlined in (1). Consequently, the equilibrium state for the deterministic model we have proposed is described as follows.

To find the disease-free equilibrium (DFE), we set the derivatives of the infected compartments ($\mathcal{I}$, $\mathcal{R}$, $\mathcal{B}$) to zero:

$$\frac{d\mathcal{I}}{dt} = 0 \Rightarrow \frac{\beta_1 \mathcal{B}(t)\mathcal{S}(t)}{\mathsf{N}(t)} + \frac{\beta_2 \mathcal{I}(t)\mathcal{S}(t)}{\mathsf{N}(t)} - (\mu + \gamma)\mathcal{I}(t) = 0,$$

$$\frac{d\mathcal{R}}{dt} = 0 \Rightarrow \gamma \mathcal{I}(t) - \mu \mathcal{R}(t) = 0,$$

$$\frac{d\mathcal{B}}{dt} = 0 \Rightarrow \eta \mathcal{I}(t) - \delta \mathcal{B}(t) = 0.$$

Since $\frac{d\mathcal{I}}{dt} = 0$, $\frac{d\mathcal{R}}{dt} = 0$, and $\frac{d\mathcal{B}}{dt} = 0$, and assuming no infection is present in the disease-free state, we have

$$\mathcal{I}(t) = 0,$$
$$\mathcal{R}(t) = 0,$$
$$\mathcal{B}(t) = 0.$$

Substituting $\mathcal{I}(t) = 0$, $\mathcal{R}(t) = 0$, and $\mathcal{B}(t) = 0$ into the equation for $\frac{d\mathcal{S}}{dt}$

$$\frac{d\mathcal{S}}{dt} = \xi - \mu \mathcal{S}(t).$$

At equilibrium, $\frac{d\mathcal{S}}{dt} = 0$, thus

$$0 = \xi - \mu \mathcal{S}^0,$$
$$\mathcal{S}^0 = \frac{\xi}{\mu}.$$

Thus, the disease-free equilibrium is

$$\mathcal{E}^0 = \left(\mathcal{S}^0, \mathcal{I}^0, \mathcal{R}^0, \mathcal{B}^0 \right) = \left(\frac{\xi}{\mu}, 0, 0, 0 \right).$$

Reproduction number

$$\mathcal{F} = \begin{bmatrix} \beta_2 & \beta_1 \\ 0 & 0 \end{bmatrix},$$

$$\mathcal{V} = \begin{bmatrix} \gamma + \mu & 0 \\ -\eta & \delta \end{bmatrix}.$$

To find $\mathbb{R}_0$, we first calculate the inverse of $\mathcal{V}$

$$\mathcal{V}^{-1} = \begin{bmatrix} \frac{1}{\gamma+\mu} & 0 \\ \frac{\eta}{\delta(\gamma+\mu)} & \frac{1}{\delta} \end{bmatrix}.$$

Multiplying $\mathcal{F}$ by $\mathcal{V}^{-1}$ gives

$$\mathcal{F}\mathcal{V}^{-1} = \begin{bmatrix} \beta_2 & \beta_1 \\ 0 & 0 \end{bmatrix} \begin{bmatrix} \frac{1}{\gamma+\mu} & 0 \\ \frac{\eta}{\delta(\gamma+\mu)} & \frac{1}{\delta} \end{bmatrix} = \begin{bmatrix} \frac{\beta_2}{\gamma+\mu} + \beta_1 \frac{\eta}{\delta(\gamma+\mu)} & \frac{\beta_1}{\delta} \\ 0 & 0 \end{bmatrix}.$$

The dominant eigenvalue of this matrix, representing $\mathbb{R}_0$, is

$$\mathbb{R}_0 = \frac{\beta_2}{\gamma+\mu} + \beta_1 \frac{\eta}{\delta(\gamma+\mu)} = \frac{1}{\gamma+\mu} \left(\beta_2 + \beta_1 \frac{\eta}{\delta} \right).$$

The threshold quantity or the basic reproduction number is (the dominant eigenvalue of the matrix $\mathcal{FV}^{-1}$)

$$\mathbb{R}_0 = \frac{1}{\gamma + \mu}\left(\beta_2 + \beta_1 \frac{\eta}{\delta}\right).\tag{2}$$

Based on the framework of [11], the disease-free equilibrium is locally asymptotically stable when $\mathbb{R}_0 < 1$ and the same fixed point will lose the stability if $\mathbb{R}_0 > 1$. Moreover, when $\mathbb{R}_0 > 1$, the model has a fixed point called the endemic equilibrium. To find the endemic equilibrium, where $\frac{dS}{dt} = 0$, $\frac{dI}{dt} = 0$, $\frac{dR}{dt} = 0$, and $\frac{dB}{dt} = 0$, we consider

$$0 = \xi - \frac{\beta_1 \mathcal{B} \mathcal{S}}{\mathsf{N}} - \frac{\beta_2 \mathcal{I} \mathcal{S}}{\mathsf{N}} - \mu \mathcal{S},$$

$$0 = \frac{\beta_1 \mathcal{B} \mathcal{S}}{\mathsf{N}} + \frac{\beta_2 \mathcal{I} \mathcal{S}}{\mathsf{N}} - (\mu + \gamma)\mathcal{I},$$

$$0 = \gamma I - \mu \mathcal{R},$$

$$0 = \eta \mathcal{I} - \delta \mathcal{B}.$$

To find the endemic equilibrium points $\mathcal{E}^* = (\mathcal{S}^*, \mathcal{I}^*, \mathcal{R}^*, \mathcal{B}^*)$ of the system, we first solve for $\mathcal{R}$ and $\mathcal{B}$ using the given relationships

$$\mathcal{R} = \frac{\gamma}{\mu}\mathcal{I},$$

$$\mathcal{B} = \frac{\eta}{\delta}\mathcal{I}.$$

Substituting these into the equations for $\mathcal{S}$ and $\mathcal{I}$, we obtain

$$0 = \xi - \frac{\beta_1\left(\frac{\eta}{\delta}\mathcal{I}\right)\mathcal{S}}{\mathsf{N}} - \frac{\beta_2 \mathcal{I} \mathcal{S}}{\mathsf{N}} - \mu \mathcal{S},$$

$$0 = \left(\frac{\beta_1 \frac{\eta}{\delta} + \beta_2}{\mathsf{N}}\right)\mathcal{I}\mathcal{S} - (\mu + \gamma)\mathcal{I}.$$

Simplifying these equations,

$$0 = \xi - \left(\frac{\beta_1 \frac{\eta}{\delta} + \beta_2}{\mathsf{N}}\right)\mathcal{I}\mathcal{S} - \mu \mathcal{S},$$

$$0 = \left(\frac{\beta_1 \frac{\eta}{\delta} + \beta_2}{\mathsf{N}}\right)\mathcal{I}\mathcal{S} - (\mu + \gamma)\mathcal{I}.$$

Isolating $\mathcal{I}$:

$$\mathcal{I}\left[\left(\frac{\beta_1 \frac{\eta}{\delta} + \beta_2}{\mathsf{N}}\right)\mathcal{S} - (\mu + \gamma)\right] = 0.$$

As $\mathcal{I} > 0$ as given, we solve for $\mathcal{S}$

$$\mathcal{S}^* = \frac{(\mu + \gamma)\mathsf{N}}{\beta_1 \frac{\eta}{\delta} + \beta_2}.$$

$$\xi = \left(\frac{\beta_1 \frac{\eta}{\delta} + \beta_2}{\mathsf{N}}\right)\mathcal{I}^* \mathcal{S}^* + \mu \mathcal{S}^*,$$

$$\mathcal{I}^* = \frac{\xi - \mu \mathcal{S}^*}{\left(\frac{\beta_1 \frac{\eta}{\delta} + \beta_2}{\mathsf{N}}\right)\mathcal{S}^*}.$$

Substituting $\mathcal{S}^*$,

$$\mathcal{I}^* = \frac{\xi(\beta_1\frac{\eta}{\delta} + \beta_2) - \mu(\mu + \gamma)\mathsf{N}}{(\mu + \gamma)(\beta_1\frac{\eta}{\delta} + \beta_2)}.$$

Finally, we compute $\mathcal{R}^*$ and $\mathcal{B}^*$ using the initial relationships:

$$\mathcal{R}^* = \frac{\gamma}{\mu}\mathcal{I}^*,$$

$$\mathcal{B}^* = \frac{\eta}{\delta}\mathcal{I}^*.$$

Hence, the endemic equilibrium points are

$$\mathcal{E}^* = (\mathcal{S}^*, \mathcal{I}^*, \mathcal{R}^*, \mathcal{B}^*).$$

This foundational understanding aids in appreciating the stochastic elements introduced to the model, as stochastic processes can then be seen as perturbations to this deterministic framework, contributing additional insights into the system's behavior under uncertainty.

3. Stochastic Model

Incorporating Lévy noise can be beneficial, particularly when the noise-scaled drift velocity scheme functions inside a threshold-valued interval. The interaction between local and non-local conditions of Lipschitz shows that inserting Lévy noise can boost shared information or bit count in various feedback illness issues that conform to random SDEs. Lévy noise has more benefits over normal Gaussian noises in mathematical models of epidemics, despite increasing mathematical complexity associated with their inclusion, as detailed in references [24,37,38]. Compared with the conventional Lévy model, the existence of jump-diffusion Lévy noise is especially useful as it offers a more precise explanation for the evolution of the membrane potential of the neuron. We next add Lévy noise to model (1), which yields the stochastic model that follows:

$$
\begin{aligned}
d\mathcal{S} &= \left[\xi - \frac{\beta_1\mathcal{B}(t)\mathcal{S}(t)}{\mathsf{N}(t)} - \frac{\beta_2\mathcal{I}(t)\mathcal{S}(t)}{\mathsf{N}(t)} - \mu\mathcal{S}(t)\right]dt + \delta_1\mathcal{S}(t)d\mathcal{W}_1(t) + \Lambda_1, \\
d\mathcal{I} &= \left[\frac{\beta_1\mathcal{B}(t)\mathcal{S}(t)}{\mathsf{N}(t)} + \frac{\beta_2\mathcal{I}(t)\mathcal{S}(t)}{\mathsf{N}(t)} - (\mu + \gamma)\mathcal{I}(t)\right]dt + \delta_2\mathcal{I}(t)d\mathcal{W}_2(t) + \Lambda_2, \\
d\mathcal{R} &= \left[\gamma\mathcal{I}(t) - \mu\mathcal{R}(t)\right]dt + \delta_3\mathcal{R}(t)d\mathcal{W}_3(t) + \Lambda_3, \\
d\mathcal{B} &= \left[\eta\mathcal{I}(t) - \delta\mathcal{B}(t)\right]dt + \delta_4\mathcal{B}(t)d\mathcal{W}_4(t) + \Lambda_4.
\end{aligned}
\tag{3}
$$

And let

$$
\begin{aligned}
\Lambda_1 &= \int_X \mathcal{Z}_1(x)S(t^-)\tilde{N}(dt, dx), \\
\Lambda_2 &= \int_X \mathcal{Z}_2(x)I(t^-)\tilde{N}(dt, dx), \\
\Lambda_3 &= \int_X \mathcal{Z}_3(x)R(t^-)\tilde{N}(dt, dx), \\
\Lambda_4 &= \int_X \mathcal{Z}_4(x)B(t^-)\tilde{N}(dt, dx).
\end{aligned}
\tag{4}
$$

$\mathcal{W}_i(t)$ for $i = 1, \cdots, 4$ are referred to as Brownian motions have biological meanings and show the addition of environmental variations. For every $i = 1, \cdots, 4$, the intensity corresponding to these noises are denoted by δ_i. , a Poisson count measure $\tilde{N}(dt, dx)$, and $Z_i, i = 1, 2, 3, 4$ represents the intensity of jump. The state transition diagram of the proposed stochastic model $\mathcal{SIRB}$ is demonstrated in Figure 2.
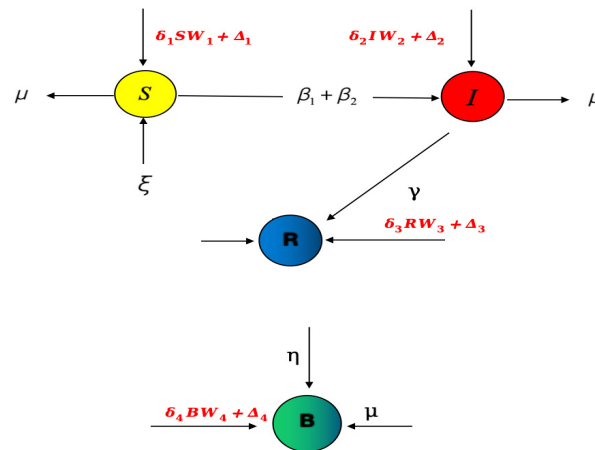
Figure 2. Flow chart of the proposed stochastic model (3).

3.1. Basic Concept

We will discuss several valuable and important concepts from nonlinear dynamics and contemporary calculus [39,40]. Consider the following initial value problem

$$dx = g(x,t)dt, \quad x(t_0) = x_0, \tag{5}$$

one can incorporate randomness into it by integrating a white noise process. In Stochastic Differential Equations (SDEs), a variable signifies random white noise, and its integral is often modeled using Brownian motion, also known as the Wiener process. This terminology honors Norbert Wiener, an American mathematician renowned for his extensive analysis of the mathematical properties of one-dimensional Brownian motion. The Wiener process represents a stochastic process with continuous temporal variation. The phrase ''Brownian motion", sometimes used interchangeably with the Wiener process, pays homage to the initial observation of this physical phenomenon by the Scottish botanist Robert Brown. Among the most popular Lévy processes, this one has applications in several disciplines, such as economics, physics, quantitative finance, applied and pure mathematics as well as in evolutionary biology. Here is a general description of an SDE

$$d\mathcal{F}(t,v) = g(X(t,v),t) + f(\mathcal{F}(t,v),t)d\mathcal{B}(t,v), \tag{6}$$

here, the notion v stands for an element of the space and the stochastic process shown by $X = X(t,v)$ with $X(0,v) = X_0$; a Lévy noise incorporates irregular fluctuations and sudden, discontinuous jumps.

3.2. Euler–Maruyama Method

The Euler–Maruyama technique is used in Ito calculus to estimate the solution of SDEs. The ideas of the Euler technique, which was originally created for ODEs, are extended to the field of SDEs by means of this method. The technique is named in honor of Gisiro Maruyama and Leonhard Euler, who were instrumental in its development. It is important to emphasize that not all deterministic approaches can benefit from this adaptation. Consider the following SDE:

$$d\mathcal{S}(t) = \alpha(\mathcal{S}(t),t)dt + \beta(\mathcal{S}(t),t)d\mathcal{F}(t), \tag{7}$$

subject to starting value $\mathcal{S}(0) = s_0$ and in the presence of Wiener process $\mathcal{F}(t)$. The main objective is to solve SDE (7) in the desired interval $[0, N]$. After the descritization of the time interval, the problem is converted into a scheme as follows:

$$\mathcal{S}_{n+1} = \mathcal{S}_n + \alpha(\mathcal{S}_n, t_n)\Delta t + \beta(\mathcal{S}_n, t_n)\Delta \mathcal{F}_n. \tag{8}$$

Here, $\mathcal{S}_n$ is the approximate value of $\mathcal{S}(t)$ at time $t_n = n\Delta t$, and $\Delta \mathcal{W}_n$ represents a portion from the Wiener process increment, often produced by multiplying a normal random variable by the value $\sqrt{\Delta t}$.

3.3. Wiener Process

The Wiener process is a countably additive function that transforms a Boolean σ-algebra of spatial subsets into independent random variables over non-overlapping sets, essentially representing a generalization of an independent increment stochastic method. This process was named to acknowledge the significance of Wiener's contributions. Exhibiting a range of distinct mathematical properties, the Wiener process stands as a pivotal concept in stochastic calculus. A key characteristic of this process is its continuous sample paths, indicating that $W(t)$ maintains continuity over time. This process follows the well-known Gaussian distribution $W(t) \; N(0, t)$ with variance t and mean of zero at any fixed time t_1. Among other properties, the distinguishing feature of the Wiener process is the independence of the statistics over non-intersecting intervals of time.

4. Positive Global Solution of the Model

In this part of the manuscript, we want to show that the suggested stochastic epidemic model with jumps has a global positive solution. We will make two assumptions, Hypothesis 1 and Hypothesis 2, to simplify our analysis. A global positive solution for the system (3) must be shown to exist and be unique, and this requires a number of assumptions.

Hypothesis 1. $\forall \; \mathcal{M} > 0 \; \exists \; \mathbb{L}_{\mathcal{M}} > 0$ *such that*

$$\int_{\mathcal{F}} |\mathcal{Q}_i(v_1, x) - \mathcal{Q}_i(v_2, x)|^2 v(dx) \le \mathbb{L}_{\mathcal{M}} |v_1 - v_2|^2, i = 1, 2, 3, 4$$

with $|w_1| \vee |w_2| \le \mathbb{M}$ *where*

$$\mathcal{Q}_1(v, x) = Z_1(x) v \text{ for } v = \mathcal{S}(t^-),$$
$$\mathcal{Q}_2(v, x) = Z_2(x) v \text{ for } v = \mathcal{I}(t^-),$$
$$\mathcal{Q}_3(v, x) = Z_3(x) v \text{ for } v = \mathcal{R}(t^-),$$
$$\mathcal{Q}_4(v, x) = Z_4(x) v \text{ for } v = \mathcal{B}(t^-).$$

Hypothesis 2. $C \ge |\log(\mathcal{Z}_i(x) + 1)|$ *for* $-1 < \mathcal{Z}_i(x),$ $\quad i = 1, \cdots, 4,$ *here* $C \in R_+$.

Theorem 1. *A solution* $(\mathcal{S}(t), \mathcal{I}(t), \mathcal{R}(t), \mathcal{B}(t))$ *of model (3) on* $t \ge 0$ *for any initial value* $(\mathcal{S}(0), \mathcal{I}(0), \mathcal{R}(0), \mathcal{B}(0)) \in \mathbb{R}_+^4$, *and the solution will remain in* $\mathbb{R}_+^4$ *with probability one, i.e., for all* $t \ge 0$, *namely,* $(\mathcal{S}(t), \mathcal{I}(t), \mathcal{R}(t), \mathcal{B}(t)) \in \mathbb{R}_+^4$.

Proof. Keeping in view assumption (Hypothesis 1), we can argue that the diffusion and drift are locally Lipschitz. This ensures that the underlying system has a unique local solution in the time interval $[0, \tau_e)$. The explosion time is denoted by the notation τ_e; readers are referred to [37,38] for a more thorough explanation. To prove the solution's global character, it suffices to show that $\tau_e = \infty$. In order to support this assertion, take into account a big enough positive real integer k_0 such that all possible solutions to the issue fall inside the interval $\left[\frac{1}{k_0}, k_0\right]$. Furthermore, assuming $k \ge k_0$, allow

$$\tau_k = inf\left\{t \in [0, \tau_e) : \frac{1}{k} \ge \min\{\mathcal{S}(t), \mathcal{I}(t), \mathcal{R}(t), \mathcal{B}(t)\}, \text{ or}\right.$$
$$k \le \max\{\mathcal{S}(t), \mathcal{I}(t), \mathcal{R}(t), \mathcal{B}(t)\}. \tag{9}$$

In this research, if $\inf \phi = \infty$, the empty set is denoted as ϕ. As $k \to \infty$, τ_k grows, according to the definition. Given that τ_∞ represents the limit of τ_k, it follows that, virtually surely, $\tau_\infty \le \tau_e$ (a.s.). Stated otherwise, we need to prove that $\tau_\infty = \infty$ a.s. Should this

claim be untrue, then there are two constants, $T > 0$ and $\epsilon \in (0, 1)$, which are associated in the following manner:

$$\epsilon < P\{\tau_\infty \leq T\}. \tag{10}$$

Consequently, we have for the value $k_0 \leq k_1$

$$P\{T \geq \tau_k\} \geq \epsilon, \ \forall \ k_1 \leq k.$$

Before we continue, let us define a Lyapunov function of the following form:

$$\begin{aligned}
\mathcal{V} &= (\mathcal{S} - c_1 \log \frac{\mathcal{S}}{c_1} - c_1) + (\mathcal{I} - 1 - \log \mathcal{I}) + (\mathcal{R} - \log \mathcal{R} - 1) \\
&\quad + (\mathcal{B} - 1 - \log \mathcal{B}),
\end{aligned} \tag{11}$$

and following that, we shall obtain the value of the constant c_1. Through the use of Itô's formula, we obtain

$$\begin{aligned}
d\mathcal{V}(\mathcal{S}, \mathcal{I}, \mathcal{R}, \mathcal{B}) &= L\mathcal{V}(\mathcal{S}, \mathcal{I}, \mathcal{R}, \mathcal{B})dt + \delta_1(\mathcal{S} - c_1)d\mathcal{W}_1(t) + \delta_2(\mathcal{I} - 1)d\mathcal{W}_2(t) \\
&\quad + \delta_3(\mathcal{R} - 1)d\mathcal{W}_3(t) + \delta_4(\mathcal{B} - 1)d\mathcal{W}_4(t) \\
&\quad + \int_{\mathcal{F}} [\mathcal{Z}_1(x)\mathcal{S} - c_1 \log(1 + \mathcal{Z}_1(x))]\tilde{N}(dt, dx) \\
&\quad + \int_{\mathcal{F}} [\mathcal{Z}_2(x)\mathcal{I} - \log(1 + \mathcal{Z}_2(x))]\tilde{N}(dt, dx) \\
&\quad + \int_{\mathcal{F}} [\mathcal{Z}_3(x)\mathcal{R} - \log(1 + \mathcal{Z}_3(x))]\tilde{N}(dt, dx) \\
&\quad + \int_{\mathcal{F}} [\mathcal{Z}_4(x)\mathcal{B} - \log(1 + \mathcal{Z}_4(x))]\tilde{N}(dt, dx).
\end{aligned} \tag{12}$$

In Equation (12), $L\mathcal{V} : \mathbb{R}_+^4 \to \mathbb{R}_+$ is defined by the following formula, and by applying condition (Hypothesis 2), we obtain

$$\begin{aligned}
L\mathcal{V} &= \left(1 - \frac{c_1}{\mathcal{S}}\right)\left(\xi - \frac{\beta_1 \mathcal{B}\mathcal{S}}{\mathsf{N}} - \frac{\beta_2 \mathcal{I}\mathcal{S}}{\mathsf{N}} - \mu\mathcal{S}\right) + \frac{c_1}{2}\delta_1^2 \\
&\quad + \left(1 - \frac{1}{\mathcal{I}}\right)\left(\frac{\beta_1 \mathcal{B}\mathcal{S}}{\mathsf{N}} + \frac{\beta_2 \mathcal{I}\mathcal{S}}{\mathsf{N}} - (\mu + \gamma)\mathcal{I}\right) + \frac{1}{2}\delta_2^2 \\
&\quad + \left(1 - \frac{1}{\mathcal{R}}\right)\left(\gamma\mathcal{I} - \mu\mathcal{R}\right) + \frac{1}{2}\delta_3^2 + \left(1 - \frac{1}{\mathcal{B}}\right)\left(\eta\mathcal{I} - \delta\mathcal{B}\right) + \frac{1}{2}\delta_4^2 \\
&= \xi - \frac{\beta_1 \mathcal{B}\mathcal{S}}{\mathsf{N}} - \frac{\beta_2 \mathcal{I}\mathcal{S}}{\mathsf{N}} - \mu\mathcal{S} - c_1\xi + \frac{c_1\beta_1\mathcal{B}}{\mathsf{N}} + \frac{c_1\beta_2\mathcal{I}}{\mathsf{N}} + c_1\mu + \frac{c_1}{2}\delta_1^2 \\
&\quad + \frac{\beta_1 \mathcal{B}\mathcal{S}}{\mathsf{N}} + \frac{\beta_2 \mathcal{I}\mathcal{S}}{\mathsf{N}} - (\mu + \gamma)\mathcal{I} - \frac{\beta_1 \mathcal{B}\mathcal{S}}{\mathcal{I}\mathsf{N}} - \frac{\beta_2 \mathcal{S}}{\mathsf{N}} + (\mu + \gamma) + \frac{1}{2}\delta_2^2 \\
&\quad + \gamma\mathcal{I} - \mu\mathcal{R} - \frac{\gamma\mathcal{I}}{\mathcal{R}} + \mu + \eta\mathcal{I} - \delta\mathcal{B} - \frac{\eta\mathcal{I}}{\mathcal{B}} + \delta + \frac{1}{2}\delta_3^2 + \frac{1}{2}\delta_4^2 \\
&\quad + \int_{\mathcal{F}} [c_1\mathcal{Z}_1(x) - c_1 \log(1 + \mathcal{Z}_1(x))]\nu(dx) + \int_{\mathcal{F}} [\mathcal{Z}_2(x) - \log(1 + \mathcal{Z}_2(x))]\nu(dx) \\
&\quad + \int_{\mathcal{F}} [\mathcal{Z}_3(x) - \log(1 + \mathcal{Z}_3(x))]\nu(dx) + \int_{\mathcal{F}} [\mathcal{Z}_4(x) - \log(1 + \mathcal{Z}_4(x))]\nu(dx).
\end{aligned} \tag{13}$$

Taking $c_1 = \frac{\delta}{\beta_1}$, such that $c_1\beta_1 - \delta = 0$. Moreover $1 \geq \mathcal{S} + \mathcal{R} + \mathcal{I}$,

$$\begin{aligned}
L\mathcal{V} &\leq \xi + c_1\mu + \beta_2 + 2\mu + \gamma + \delta + \frac{c_1}{2}\delta_1^2 + \frac{1}{2}\delta_2^2 + \frac{1}{2}\delta_3^2 + \frac{1}{2}\delta_4^2 \\
&\quad + \int_{\mathcal{F}} [c_1\mathcal{Z}_1(x) - c_1 \log(1 + \mathcal{Z}_1(x))]\nu(dx) + \int_{\mathcal{F}} [\mathcal{Z}_2(x) - \log(1 + \mathcal{Z}_2(x))]\nu(dx) \\
&\quad + \int_{\mathcal{F}} [\mathcal{Z}_3(x) - \log(1 + \mathcal{Z}_3(x))]\nu(dx) + \int_{\mathcal{F}} [\mathcal{Z}_4(x) - \log(1 + \mathcal{Z}_4(x))]\nu(dx). = K.
\end{aligned} \tag{14}$$

As a result, for Theorem 1 , the proof structure is substantially the same as that of [37]. Therefore, the proof of the theorem is completed by removing the unnecessary steps. □

5. Extinction

It is widely acceptable that an epidemic must be eradicated gradually by determining the right conditions and implementing proper strategies, which may be found by examining the behavior of the infectious illness. We shall examine necessary criteria for disease extinction in the stochastic model in this section. It is necessary to determine the stochastic threshold prior to examining the dynamics of the stochastic epidemic model with jumps (3). The expression for the threshold quantity $\mathbb{R}_s$ is as follows:

$$\mathbb{R}_s = \frac{\frac{\beta_1 \eta}{\delta} + \beta_2}{\left(\mu + \gamma + \frac{\lambda_2^2}{2} + \int_{\mathcal{F}} [\mathcal{Z}_2(x) - \log(1 + \mathcal{Z}_2(x))] \nu(dx) \right)}. \tag{15}$$

The notion presented below is worthy of use in subsequent parts of the paper:

$$\langle \mathcal{H}(t) \rangle = \frac{1}{t} \int_0^t \mathcal{H}(s) ds. \tag{16}$$

Lemma 1. *If for system* (3) *$(\mathcal{S}, \mathcal{I}, \mathcal{R}, \mathcal{B})$ is a solution with initial conditions $(\mathcal{S}(0), \mathcal{I}(0), \mathcal{R}(0), \mathcal{B}(0))$ $\in \mathbb{R}_+^4$, then a.s.,*

$$\lim_{t \to \infty} \frac{\mathcal{S}(t) + \mathcal{I}(t) + \mathcal{R}(t) + \mathcal{B}(t)}{t} = 0. \tag{17}$$

Moreover, if $\mu > \frac{(\delta_1^2 \vee \delta_2^2 \vee \delta_3^2 \vee \delta_4^2)}{2}$, then

$$\begin{aligned}
\lim_{t \to \infty} \frac{\int_0^t \mathcal{S}(s) d\mathcal{Z}_1(s)}{t} &= 0, \\
\lim_{t \to \infty} \frac{\int_0^t \mathcal{I}(u) d\mathcal{Z}_2(u)}{t} &= 0, \\
\lim_{t \to \infty} \frac{\int_0^t \mathcal{R}(s) d\mathcal{Z}_3(s)}{t} &= 0, \\
\lim_{t \to \infty} \frac{\int_0^t \mathcal{B}(s) d\mathcal{Z}_4(s)}{t} &= 0, \ a.s.
\end{aligned} \tag{18}$$

Then, the solution of system (3)

$$\begin{aligned}
\limsup_{t \to \infty} \mathcal{S}(t) &= \frac{\xi}{\mu}, \\
\limsup_{t \to \infty} \mathcal{I}(t) &= 0, \\
\limsup_{t \to \infty} \mathcal{R}(t) &= 0, \\
\limsup_{t \to \infty} \mathcal{B}(t) &= 0, \ a.s.
\end{aligned} \tag{19}$$

Proof. From the system (3), we can have

$$d(\mathcal{S} + \mathcal{I} + \mathcal{R} + \mathcal{B}) = \xi - \mu(\mathcal{S} + \mathcal{I} + \mathcal{R}) - \delta\mathcal{B} - +\delta_1 \mathcal{S} d\mathcal{W}_1 + \delta_2 \mathcal{I} d\mathcal{W}_2 + \delta_3 \mathcal{R} d\mathcal{W}_3 + \delta_4 \mathcal{B} d\mathcal{W}_4.$$

Solving this equation, we can obtain

$$\mathcal{S}(t) + \mathcal{I}(t) + \mathcal{R}(t) + \mathcal{B}(t) = \frac{\xi}{\mu} + \left(\mathcal{S}(0) + \mathcal{I}(0) + \mathcal{R}(0) - \frac{xi}{\mu}\right)e^{-\mu t} - (\mathcal{B}(0) - \frac{1}{\delta})e^{-\mu t}$$

$$+ \delta_1 \int_0^t \mathcal{S}(u)e^{-\mu(t-u)}d\mathcal{W}_1(u) + \delta_2 \int_0^t \mathcal{I}(u)e^{-\mu(t-u)}d\mathcal{W}_2(u) \qquad (20)$$

$$+ \delta_3 \int_0^t \mathcal{R}(u)e^{-\mu(t-u)}d\mathcal{W}_3(u) + \delta_4 \int_0^t \mathcal{B}(u)e^{-\delta(t-u)}d\mathcal{W}_4(u).$$

Define

$$X(t) = X(0) + A(t) - Q(t) + M(t),$$

where

$$X(0) = \mathcal{S}(0) + \mathcal{I}(0) + \mathcal{R}(0) + \mathcal{B}(0),$$

$$A(t) = \frac{\xi}{\mu}(1 - e^{-\mu t}),$$

$$Q(t) = (\mathcal{S}(0) + \mathcal{I}(0) + \mathcal{R}(0))(1 - e^{-\mu t}) + \mathcal{B}(0))(1 - e^{-\delta t}),$$

$$M(t) = \delta_1 \int_0^t \mathcal{S}(u)e^{-\mu(t-u)}d\mathcal{W}_1(u) + \delta_2 \int_0^t I(u)e^{-\mu(t-u)}d\mathcal{W}_2(u)$$

$$+ \delta_3 \int_0^t \mathcal{R}(u)e^{-\mu(t-u)}d\mathcal{W}_3(u) + \delta_4 \int_0^t \mathcal{B}(u)e^{-\delta(t-u)}d\mathcal{W}_4(u).$$

$M(t)$ is a continuous local martingale with $M(0) = 0$. From (20), we have $\mathcal{S}(t) + \mathcal{I}(t) + \mathcal{R}(t) + \mathcal{B}(t) \leq X(t)$ a.s. $\forall t > 0$. One can see that $A(t)$ and $Q(t)$ are continuous adapted increasing processes on $t \geq 0$ with $A(0) = Q(0)$. From large number theorem for the martingale in [41], we can obtain that $\lim_{t\to\infty} X(t) < \infty$ a.s. Hence

$$\limsup_{t\to\infty}(\mathcal{S}(t) + \mathcal{I}(t) + \mathcal{R}(t) + \mathcal{B}(t)) < \infty, \text{ a.s.} \qquad (21)$$

In view of above inequality, we can easily obtain

$$\lim_{t\to\infty}\frac{\mathcal{S}(t)}{t} = 0, \quad \lim_{t\to\infty}\frac{I(t)}{t} = 0, \quad \lim_{t\to\infty}\frac{\mathcal{R}(t)}{t} = 0, \quad \lim_{t\to\infty}\frac{\mathcal{B}(t)}{t} = 0, \quad \text{a.s.}$$

Set

$$M_1(t) = \int_0^t \mathcal{S}(u)\,d\mathcal{W}_1(u), \quad M_2(t) = \int_0^t I(u)\,d\mathcal{W}_2(u),$$

$$M_3(t) = \int_0^t \mathcal{R}(u)\,d\mathcal{W}_3(u), \quad M_4(t) = \int_0^t B(u)\,d\mathcal{W}_4(u).$$

Due to the quadratic variations, we can have

$$\langle M_1(t), M_1(t)\rangle = \int_0^t \mathcal{S}^2(u)\,du \leq \left(\sup_{t\geq 0}\mathcal{S}^2(t)\right)t.$$

By the large number theorem for martingales and these quadratic variations, we can obtain

$$\lim_{t\to\infty}\frac{\int_0^t \mathcal{S}(u)\,d\mathcal{W}_1(u)}{t} = 0, \quad \lim_{t\to\infty}\frac{\int_0^t \mathcal{I}(u)\,d\mathcal{W}_2(u)}{t} = 0,$$

$$\lim_{t\to\infty}\frac{\int_0^t \mathcal{R}(u)\,d\mathcal{W}_3(u)}{t} = 0, \quad \lim_{t\to\infty}\frac{\int_0^t \mathcal{B}(u)\,d\mathcal{W}_4(u)}{t} = 0, \text{a.s.}$$

This finishes the proof. $\square$

Theorem 2. *Assume that $(\mathcal{S}(t), \mathcal{I}(t), \mathcal{R}(t), \mathcal{B}(t))$ correspond to initial data $(\mathcal{S}, \mathcal{I}, \mathcal{Q}, \mathcal{R}, \mathcal{B})(0) \in \mathbb{R}^4_+$ be a solution of model (3). Further, if $\mathbb{R}_s < 1$, then such a solution of system (3) satisfies the following relations:*

$$
\begin{aligned}
\lim_{t \to \infty} \langle \mathcal{S}(t) \rangle &= \frac{\Pi}{\mu}, \ \ a.s., \\
\lim_{t \to \infty} \langle \mathcal{I}(t) \rangle &= 0, \ \ a.s., \\
\lim_{t \to \infty} \langle \mathcal{R}(t) \rangle &= 0, \ \ a.s., \\
\lim_{t \to \infty} \langle \mathcal{B}(t) \rangle &= 0, \ \ a.s.
\end{aligned}
\tag{22}
$$

This suggests that eventually the virus inside the population will undoubtedly be eliminated.

Proof. By integrating the system (3), we were able to obtain the following set of equations:

$$
\begin{aligned}
\frac{(\mathcal{S}(t) - \mathcal{S}(0))}{t} &= \xi - \frac{\beta_1 \langle \mathcal{BS} \rangle}{\langle \mathsf{N} \rangle} - \frac{\beta_2 \langle \mathcal{IS} \rangle}{\langle \mathsf{N} \rangle} - \mu \langle \mathcal{S} \rangle + \frac{\delta_1 \int_0^t \mathcal{S}(r) d\mathcal{W}_1(r)}{t}, \\
&\quad + \frac{1}{t} \int_0^t \left[\int_{\mathcal{F}} \mathcal{Z}_1(x) \mathcal{S}(t^-) \tilde{\mathsf{N}}(dt, dx) \right] dr, \\
\frac{(\mathcal{I}(t) - \mathcal{I}(0))}{t} &= \frac{\beta_1 \langle \mathcal{BS} \rangle}{\langle \mathsf{N} \rangle} - \frac{\beta_2 \langle \mathcal{IS} \rangle}{\langle \mathsf{N} \rangle} - (\mu + \gamma) \langle \mathcal{I} \rangle + \frac{\delta_2 \int_0^t \mathcal{I}(r) \mathcal{W}_2(r)}{t}, \\
&\quad + \frac{1}{t} \int_0^t \left[\int_{\mathcal{F}} \mathcal{Z}_2(x) \mathcal{I}(t^-) \tilde{\mathsf{N}}(dt, dx) \right] dr, \\
\frac{(\mathcal{R}(t) - \mathcal{R}(0))}{t} &= \gamma \langle \mathcal{I} \rangle - \mu \langle \mathcal{R} \rangle + \frac{\delta_3 \int_0^t \mathcal{R}(r) d\mathcal{W}_3(r)}{t}, \\
&\quad + \frac{1}{t} \int_0^t \left[\int_{\mathcal{F}} \mathcal{Z}_3(x) \mathcal{R}(t^-) \tilde{\mathsf{N}}(dt, dx) \right] dr, \\
\frac{(\mathcal{B}(t) - \mathcal{B}(0))}{t} &= \eta \langle \mathcal{I} \rangle - \delta \langle \mathcal{B} \rangle + \frac{\delta_4 \int_0^t \mathcal{B}(r) d\mathcal{W}_4(r)}{t}. \\
&\quad + \frac{1}{t} \int_0^t \left[\int_{\mathcal{F}} \mathcal{Z}_4(x) \mathcal{B}(t^-) \tilde{\mathsf{N}}(dt, dx) \right] dr,
\end{aligned}
\tag{23}
$$

Considering the second-to-last relation of the aforementioned system, we obtain

$$
\begin{aligned}
\langle \mathcal{B} \rangle &= \frac{\eta}{\delta} \langle \mathcal{I} \rangle - \frac{1}{\delta} \left(\frac{\mathcal{B}(t) - \mathcal{B}(0)}{t} \right) + \frac{\delta_4}{\delta} \left(\frac{\int_0^t \mathcal{B}(r) d\mathcal{W}_4(r)}{t} \right) + \int_{\mathcal{F}} [\log(1 + \mathcal{Z}_4(x))] \tilde{\mathsf{N}}(dt, dx), \\
&= \frac{\eta}{\delta} \langle \mathcal{I} \rangle + \mathcal{M}_1(t),
\end{aligned}
\tag{24}
$$

where

$$
\mathcal{M}_1(t) = -\frac{1}{\delta} \left(\frac{\mathcal{B}(t) - \mathcal{B}(0)}{t} \right) + \frac{\delta_4}{\delta} \left(\frac{\int_0^t \mathcal{B}(r) d\mathcal{W}_4(r)}{t} \right) + \int_{\mathcal{F}} [\log(1 + \mathcal{Z}_4(x))] \tilde{\mathsf{N}}(dt, dx).
\tag{25}
$$

Direct application of the *Itô* formula to $\mathcal{V} = \log \mathcal{I}(t)$ yields the following outcomes:

$$
d\log \mathcal{I}(t) = \mathcal{LV} dt + \delta_2 d\mathcal{W}_2(t) + \int_{\mathcal{F}} [\log(1 + \mathcal{Z}_2(x))] \tilde{\mathsf{N}}(dt, dx).
\tag{26}
$$

where

$$
\mathcal{LV} = \left[\frac{\beta_1 \mathcal{BS}}{\mathcal{IN}} + \frac{\beta_2 \mathcal{S}}{\mathsf{N}} - (\mu + \gamma) - \frac{\delta_2^2}{2} \right] dt - \int_{\mathcal{F}} [\mathcal{Z}_2(x) - \log(1 + \mathcal{Z}_2(x))] \nu(dx).
\tag{27}
$$

Then, Equation (26) becomes

$$
\begin{aligned}
d \log \mathcal{I} &= \left[\frac{\beta_1 \mathcal{B} \mathcal{S}}{\mathcal{I} \mathsf{N}} + \frac{\beta_2 \mathcal{S}}{\mathsf{N}} - (\mu + \gamma) - \frac{\delta_2^2}{2} \right] dt - \int_{\mathcal{F}} [\mathcal{Z}_2(x) - \log(1 + \mathcal{Z}_2(x))] \nu(dx) \\
&\quad + \delta_2 d\mathcal{W}_2(t) + \int_{\mathcal{F}} [\log(1 + \mathcal{Z}_2(x))] \tilde{\mathsf{N}}(dt, dx), \\
&\leq \left[\frac{\beta_1 \mathcal{B}}{\mathcal{I}} + \beta_2 - (\mu + \gamma) - \frac{\delta_2^2}{2} \right] dt - \int_{\mathcal{F}} [\mathcal{Z}_2(x) - \log(1 + \mathcal{Z}_2(x))] \nu(dx) \\
&\quad + \delta_2 d\mathcal{W}_2(t) + \int_{\mathcal{F}} [\log(1 + \mathcal{Z}_2(x))] \tilde{\mathsf{N}}(dt, dx).
\end{aligned}
\tag{28}
$$

From 0 to t, one can easily integrate Equation (28) and divide the result by t to obtain the following relation:

$$
\begin{aligned}
\frac{\log \mathcal{I} - \log \mathcal{I}(0)}{t} &\leq \left[\frac{\beta_1 \langle \mathcal{B} \rangle}{\langle \mathcal{I} \rangle} + \beta_2 - (\mu + \gamma + \frac{\lambda_2^2}{2}) - \int_{\mathcal{F}} [\mathcal{Z}_2(x) - \log(1 + \mathcal{Z}_2(x))] \nu(dx) \right] \\
&\quad + \frac{\delta_2 d\mathcal{W}_2(t)}{t} + \frac{\int_{\mathcal{F}} [\log(1 + \mathcal{Z}_2(x))] \tilde{\mathsf{N}}(dt, dx)}{t}.
\end{aligned}
\tag{29}
$$

If we substitute relation (24) in Equation (29), we have the following expression:

$$
\begin{aligned}
\frac{\log \mathcal{I}(t)}{t} &\leq \left[\frac{\beta_1 (\frac{\eta}{\delta} \langle \mathcal{I} \rangle + \mathcal{M}_1(t))}{\langle \mathcal{I} \rangle} + \beta_2 - (\mu + \gamma + \frac{\lambda_2^2}{2}) - \int_{\mathcal{F}} [\mathcal{Z}_2(x) - \log(1 + \mathcal{Z}_2(x))] \nu(dx) \right] \\
&\quad + \frac{\log \mathcal{I}(0)}{t} + \frac{\delta_2 d\mathcal{W}_2(t)}{t} + \frac{\int_{\mathcal{F}} [\log(1 + \mathcal{Z}_2(x))] \tilde{\mathsf{N}}(dt, dx)}{t} \\
&\leq \left[\frac{\frac{\beta_1 \eta}{\delta} \langle \mathcal{I} \rangle}{\langle \mathcal{I} \rangle} + \beta_2 - (\mu + \gamma + \frac{\lambda_2^2}{2}) - \int_{\mathcal{F}} [\mathcal{Z}_2(x) - \log(1 + \mathcal{Z}_2(x))] \nu(dx) \right] \\
&\quad + \frac{\beta_1 \mathcal{M}_1(t)}{\langle \mathcal{I} \rangle} + \frac{\log \mathcal{I}(0)}{t} + \frac{\delta_2 d\mathcal{W}_2(t)}{t} + \frac{\int_{\mathcal{F}} [\log(1 + \mathcal{Z}_2(x))] \tilde{\mathsf{N}}(dt, dx)}{t} \\
&= \left[\frac{\beta_1 \eta}{\delta} + \beta_2 - (\mu + \gamma + \frac{\lambda_2^2}{2}) - \int_{\mathcal{F}} [\mathcal{Z}_2(x) - \log(1 + \mathcal{Z}_2(x))] \nu(dx) \right] \\
&\quad + \frac{\beta_1 \mathcal{M}_1(t)}{\langle \mathcal{I} \rangle} + \frac{\log \mathcal{I}(0)}{t} + \frac{\delta_2 d\mathcal{W}_2(t)}{t} + \frac{\int_{\mathcal{F}} [\log(1 + \mathcal{Z}_2(x))] \tilde{\mathsf{N}}(dt, dx)}{t}.
\end{aligned}
\tag{30}
$$

Further, $\mathcal{M}_i(t) = \frac{\delta_i}{t} \int_0^t g_i d\mathcal{W}_i(t) + \frac{\int_{\mathcal{F}} [\log(1 + \mathcal{Z}_i(x))] \tilde{\mathsf{N}}(dt, dx)}{t}$ for $i = 1, 2, \cdots 4. g_1 = \mathcal{S}, g_2 = \mathcal{I}, g_3 = \mathcal{R}, g_4 = \mathcal{B}$ are the continuous local martingale functions and equals 0 at $t = 0$. If we let $t \to \infty$ and use Lemma 1, we obtain

$$
\limsup_{t \to \infty} \frac{1}{t} \mathcal{M}_i(t) = 0.
\tag{31}
$$

We may readily deduce that $\lim_{t \to \infty} \sup \mathcal{M}_1(t) = 0$ by using a similar reasoning. With $\mathbb{R}_s < 1$ assumed, Equation (30) becomes

$$
\limsup_{t \to \infty} \frac{\log \mathcal{I}(t)}{t} \leq \left(\mu + \gamma + \frac{\lambda_2^2}{2} + \int_{\mathcal{F}} [\mathcal{Z}_2(x) - \log(1 + \mathcal{Z}_2(x))] \nu(dx) \right) \left(\mathbb{R}_s - 1 \right) < 0, \text{ a.s.}
\tag{32}
$$

By virtue of relation (32), we have

$$
\lim_{t \to \infty} \langle \mathcal{I} \rangle = 0, \text{ a.s.}
\tag{33}
$$

Assuming relation (33) in Equation (24) and utilizing the fact $\lim_{t\to\infty} \sup \mathcal{M}_1(t) = 0$, we obtain

$$\lim_{t\to\infty} \langle \mathcal{B} \rangle = 0, \quad \text{a.s,} \tag{34}$$

Likewise, we obtain

$$\lim_{t\to\infty} \langle \mathcal{R}(t) \rangle = 0, \quad \text{a.s.} \tag{35}$$

Finally, considering the system's initial Equation (23), through the application of the relationships (34) and (35), we integrate from 0 to t and divide the result by t to obtain

$$\lim_{t\to\infty} \langle \mathcal{S} \rangle = \frac{\xi}{\mu} \quad \text{a.s.} \tag{36}$$

This completes the proof. $\square$

6. Persistence of the Disease

This section is devoted to analyzing the disease's persistence. First, we review the meaning of persistence in mean as stated in [37,38].

Definition 1 ([37,38])**.** *The model's persistence or durability will be guaranteed by the following conditions*

$$\liminf_{t\to\infty} \frac{1}{t} \int_0^t \mathcal{G}(r)dr > 0 \quad a.s. \tag{37}$$

The function $G(r)$ represents the growth rate of the disease. As mentioned in [25,26], in order to evaluate the disease's persistence, we also need to take into account the following lemmas.

Lemma 2 (Strong Law [24,37])**.** *If for a real valued and continuous $\mathcal{Y} = \{\mathcal{Y}\}_{0\leq t} \, \exists$ a local martingale $\ni$ at $t \to 0$ vanishes then*

$$\lim_{t\to\infty} \langle \mathcal{Y}, \mathcal{Y} \rangle_t = \infty, \ a.s., \ \Rightarrow \ \lim_{t\to\infty} \frac{\mathcal{Y}_t}{\langle \mathcal{Y}, \mathcal{Y} \rangle_t} = 0, \ a.s.$$

$$\limsup_{t\to\infty} \frac{\langle \mathcal{Y}, \mathcal{Y} \rangle_t}{t} < 0, \ a.s., \ \Rightarrow \ \lim_{t\to\infty} \frac{\mathcal{Y}_t}{t} = 0, \ a.s. \tag{38}$$

Lemma 3. *Suppose $h \in \mathcal{C}([0,\infty) \times \Omega, (0,\infty))$ and $\mathcal{H} \in \mathcal{C}([0,\infty) \times \Omega, \mathbb{R}) \ni \lim_{t\to\infty} \frac{\mathcal{H}(t)}{t} = 0$, a.s. If $\forall \, t \geq 0$*

$$\log h(t) \geq \lambda_0 t - \lambda \int_0^t h(s)ds + \mathcal{H}(t), a.s.$$

Then

$$\liminf_{t\to\infty} \langle h(t) \rangle \geq \frac{\lambda_0}{\lambda} a.s.$$

where $\{\lambda, \lambda_0 \in \mathbb{R} \ni \lambda > 0 \ \& \ \lambda_0 \geq 0\}$.

The prerequisites for the system (3) to persist in the mean will now be discussed. The finding summarizes the main conclusions of this ongoing investigation.

Theorem 3. *If $\mathbb{R}_0^s > 1$, then for any initial value $(\mathcal{S}_0, , \mathcal{I}_0, \mathcal{R}_0, \mathcal{B}_0) \in \mathbb{R}_+^4$, the disease $\mathcal{I}(t)$ and $\mathcal{B}(t)$ has the axiom*

$$\liminf_{t\to\infty} \langle (\mathcal{B}(t) + \mathcal{I}(t)) \rangle \geq \frac{2\xi\beta_2 \sqrt{\mathbb{R}_0^s} - 1)}{\mathcal{C}_1 \beta} \quad a.s., \tag{39}$$

where $\mathcal{C}_1 = \dfrac{\xi\beta}{\left(\mu+d+\frac{\alpha_1^2}{2}+\int_X[Z_1(x)-\log(1+Z_1(x))]\nu(dx)\right)}$ *, then we can say the disease will prevail.*

Let us define

$$\mathbb{R}_0^s = \frac{\xi\beta_2}{\left\{a_1 + \frac{\alpha_1^2}{2} + \int_X[Z_1(x) - \log(1 + Z_1(x))]\nu(dx)\right\}\left\{b_1 + \int_{\mathcal{F}}[\mathcal{Z}_2(x) - \log(1 + \mathcal{Z}_2(x))]\nu(dx)\right\}}. \tag{40}$$

where $a_1 = (d + \mu)$ and $b_1 = (\mu + \gamma + \frac{\delta_2^2}{2})$.

Proof. Set

$$\mathcal{H}_1 = -\mathcal{C}_1 ln\mathcal{S} - \mathcal{C}_2 ln\mathcal{I}, \tag{41}$$

here the unknown real numbers C_1 and C_2 will be calculated at later stages.

By using the *Itô* formula to Equation (41), we obtain

$$\begin{aligned}
d\mathsf{H}_1 &= \mathcal{L}\mathsf{H}_1 - \mathsf{C}_1\delta_1 d\mathcal{W}_1(t) - \mathsf{C}_2\delta_2 d\mathcal{W}_2(t) \\
&\quad - \mathsf{C}_1\int_{\mathcal{F}}[\mathcal{Z}_1(x)\mathcal{S} - \log(1 + \mathcal{Z}_1(x))]\tilde{\mathsf{N}}(dt,dx) - \mathsf{C}_2\int_{\mathcal{F}}[\mathcal{Z}_2(x)\mathcal{I} - \log(1 + \mathcal{Z}_2(x))]\tilde{\mathsf{N}}(dt,dx),
\end{aligned} \tag{42}$$

where

$$\begin{aligned}
\mathcal{L}\mathsf{H}_1 &= -\mathsf{C}_1\mathcal{L}(ln\mathcal{S}) - \mathsf{C}_2\mathcal{L}(ln\mathcal{I}) \\
&= -\frac{\mathsf{C}_1\xi}{\mathcal{S}} + \frac{\mathsf{C}_1\beta_1\mathcal{B}}{\mathsf{N}} + \frac{\mathsf{C}_1\beta_2\mathcal{I}}{\mathsf{N}} + \mathsf{C}_1\mu + \mathsf{C}_1\left\{\frac{\delta_1^2}{2} + \int_{\mathcal{F}}[\mathcal{Z}_1(x) - \log(1 + \mathcal{Z}_1(x))]\nu(dx)\right\} \\
&\quad - \frac{\mathsf{C}_2\beta_1\mathcal{B}\mathcal{S}}{\mathsf{N}\mathcal{I}} - \frac{\mathsf{C}_2\beta_2\mathcal{S}}{\mathsf{C}_2\mathsf{N}(t)} + \mathsf{C}_2(\mu + \gamma) + \mathsf{C}_2\left\{\frac{\delta_2^2}{2} + \int_{\mathcal{F}}[\mathcal{Z}_2(x) - \log(1 + \mathcal{Z}_2(x))]\nu(dx)\right\} \\
&\leq -\frac{\mathsf{C}_1\xi}{\mathcal{S}} - \frac{\mathsf{C}_2\beta_2\mathcal{S}}{\mathsf{C}_2\mathsf{N}(t)} + \mathsf{C}_1\left[\mu + d + \frac{\alpha_1^2}{2} + \int_X[Z_1(x) - \log(1 + Z_1(x))]\nu(dx)\right] \\
&\quad + \mathsf{C}_2\left\{\mu + \gamma + \frac{\delta_2^2}{2} + \int_{\mathcal{F}}[\mathcal{Z}_2(x) - \log(1 + \mathcal{Z}_2(x))]\nu(dx)\right\} + \frac{\mathsf{C}_1\beta_1\mathcal{B}}{\mathsf{N}} + \frac{\mathsf{C}_1\beta_2\mathcal{I}}{\mathsf{N}} \\
&\leq -2\sqrt{\mathsf{C}_1\mathsf{C}_2\xi\beta_2} + \mathsf{C}_1\left[\mu + d + \frac{\alpha_1^2}{2} + \int_X[Z_1(x) - \log(1 + Z_1(x))]\nu(dx)\right] \\
&\quad + \mathsf{C}_2\left\{\mu + \gamma + \frac{\delta_2^2}{2} + \int_{\mathcal{F}}[\mathcal{Z}_2(x) - \log(1 + \mathcal{Z}_2(x))]\nu(dx)\right\} + \mathsf{C}_1\beta_1\mathcal{B} + \mathsf{C}_1\beta_2\mathcal{I},
\end{aligned} \tag{43}$$

let $\beta = max\{\beta_1, \beta_2\}$,

$$\begin{aligned}
\mathsf{C}_1 &= \frac{\mathsf{C}_2\xi\beta_2}{\left\{\mu + d + \frac{\alpha_1^2}{2} + \int_X[Z_1(x) - \log(1 + Z_1(x))]\nu(dx)\right\}}, \\
\mathsf{C}_2 &= \frac{\mathsf{C}_2\xi\beta_2}{\left\{\mu + \gamma + \frac{\delta_2^2}{2} + \int_{\mathcal{F}}[\mathcal{Z}_2(x) - \log(1 + \mathcal{Z}_2(x))]\nu(dx)\right\}}.
\end{aligned} \tag{44}$$

Let $\beta = max\{\beta_1, \beta_2\}$, and

$$\begin{aligned}
x &= \left\{\mu + d + \frac{\alpha_1^2}{2} + \int_X[Z_1(x) - \log(1 + Z_1(x))]\nu(dx)\right\}, \\
y &= \left\{\mu + \gamma + \frac{\delta_2^2}{2} + \int_{\mathcal{F}}[\mathcal{Z}_2(x) - \log(1 + \mathcal{Z}_2(x))]\nu(dx)\right\}.
\end{aligned}$$

$$\mathcal{L}\mathsf{H}_1 \leq -2\sqrt{\frac{(\xi\beta_2)^2\xi\beta_2}{xy}} + 2\xi\beta_2 + \mathsf{C}_1\beta\big[\mathcal{B}(t) + \mathcal{I}(t)\big]$$

$$= -2\xi\beta_2\left[\sqrt{\frac{\xi\beta_2}{xy}} - 1\right] + \mathsf{C}_1\beta\big[\mathcal{B}(t) + \mathcal{I}(t)\big] \tag{45}$$

$$= -2\xi\beta_2\left[\sqrt{\mathbb{R}_0^s} - 1\right] + \mathsf{C}_1\beta\big[\mathcal{B}(t) + \mathcal{I}(t)\big].$$

Equation (45) is substituted for Equation (41), and both sides of the stochastic hepatitis B model (3) are then integrated, so we have

$$\frac{\mathsf{H}_1(\mathcal{S}(t), I(t)) - \mathsf{H}_1(\mathcal{S}(0), \mathcal{I}(0))}{t} \leq -2\xi\beta_2\left[\sqrt{\mathbb{R}_0^s} - 1\right] + \mathsf{C}_1\beta\big[\langle(\mathcal{B}(t) + \mathcal{I}(t))\rangle\big]$$

$$- \frac{\mathsf{C}_1\delta_1^2\mathcal{W}_1(t)}{t} - \frac{\mathsf{C}_2\delta_2^2\mathcal{B}_2(t)}{t}$$

$$- \frac{\mathsf{C}_1\int_{\mathcal{F}}[\mathcal{Z}_1(x)\mathcal{S} - \log(1 + \mathcal{Z}_1(x))]\tilde{\mathsf{N}}(dt, dx)}{t} \tag{46}$$

$$- \frac{\mathsf{C}_2\int_{\mathcal{F}}[\mathcal{Z}_2(x)\mathcal{A} - \log(1 + \mathcal{Z}_2(x))]\tilde{\mathsf{N}}(dt, dx)}{t},$$

$$\leq -2\xi\beta_2\left[\sqrt{\mathbb{R}_0^s} - 1\right] + \mathsf{C}_1\beta\big[\langle(\mathcal{B}(t) + \mathcal{I}(t))\rangle\big] + \Psi(t),$$

where $\Psi(t) = -\frac{\mathsf{C}_1\int_{\mathcal{F}}[\mathcal{Z}_1(x)\mathcal{S} - \log(1 + \mathcal{Z}_1(x))]\tilde{\mathsf{N}}(dt, dx)}{t} - \frac{\mathsf{C}_2\int_{\mathcal{F}}[\mathcal{Z}_2(x)\mathcal{A} - \log(1 + \mathcal{Z}_2(x))]\tilde{\mathsf{N}}(dt, dx)}{t}$.
From strong law as stated in Lemma 2, we arrive at

$$\lim_{t \to \infty} \Psi(t) = 0, \tag{47}$$

From Equation (46), we have

$$\langle(\mathcal{B}(t) + \mathcal{I}(t))\rangle \geq \frac{2\xi\beta_2(\sqrt{\mathbb{R}_0^s} - 1)}{\mathsf{C}_1\beta} - \frac{1}{\mathsf{C}_1\beta}\Psi(t) + \frac{1}{\mathsf{C}_1\beta}\left(\frac{\mathsf{H}_1(\mathcal{S}(t), I(t)) - \mathsf{H}_1(\mathcal{S}(0), \mathcal{I}(0))}{t}\right). \tag{48}$$

According to Lemma 3 and Equation (47), the limit superior of Equation (6), we have

$$\liminf_{t \to \infty} \langle(\mathcal{B}(t) + \mathcal{I}(t))\rangle \geq \frac{2\xi\beta(\sqrt{\mathbb{R}_0^s} - 1)}{\mathsf{C}_1\beta} \quad \text{a.s,} \tag{49}$$

and likewise for $\liminf_{t \to \infty} \langle B(t) + \mathcal{I}(t)\rangle \geq 0$.
Finally, the proof of Theorem (3) is concluded. □

7. Numerical Scheme and Simulations

Determining suitable parameter values is crucial for empirically validating the theoretical results associated with system (3). To achieve this, two sets of parameter values are being considered, along with the initial population numbers of bacteria and humans.

It is to be noted that the black line on the graphs represents the cumulative average of a particular variable over time throughout the simulations. This line provides insights into the overall trend and the long-term behavior of the variable, smoothing out short-term fluctuations to highlight more sustained patterns. This kind of average is useful for identifying underlying trends in data that are otherwise too erratic or noisy to analyze directly.

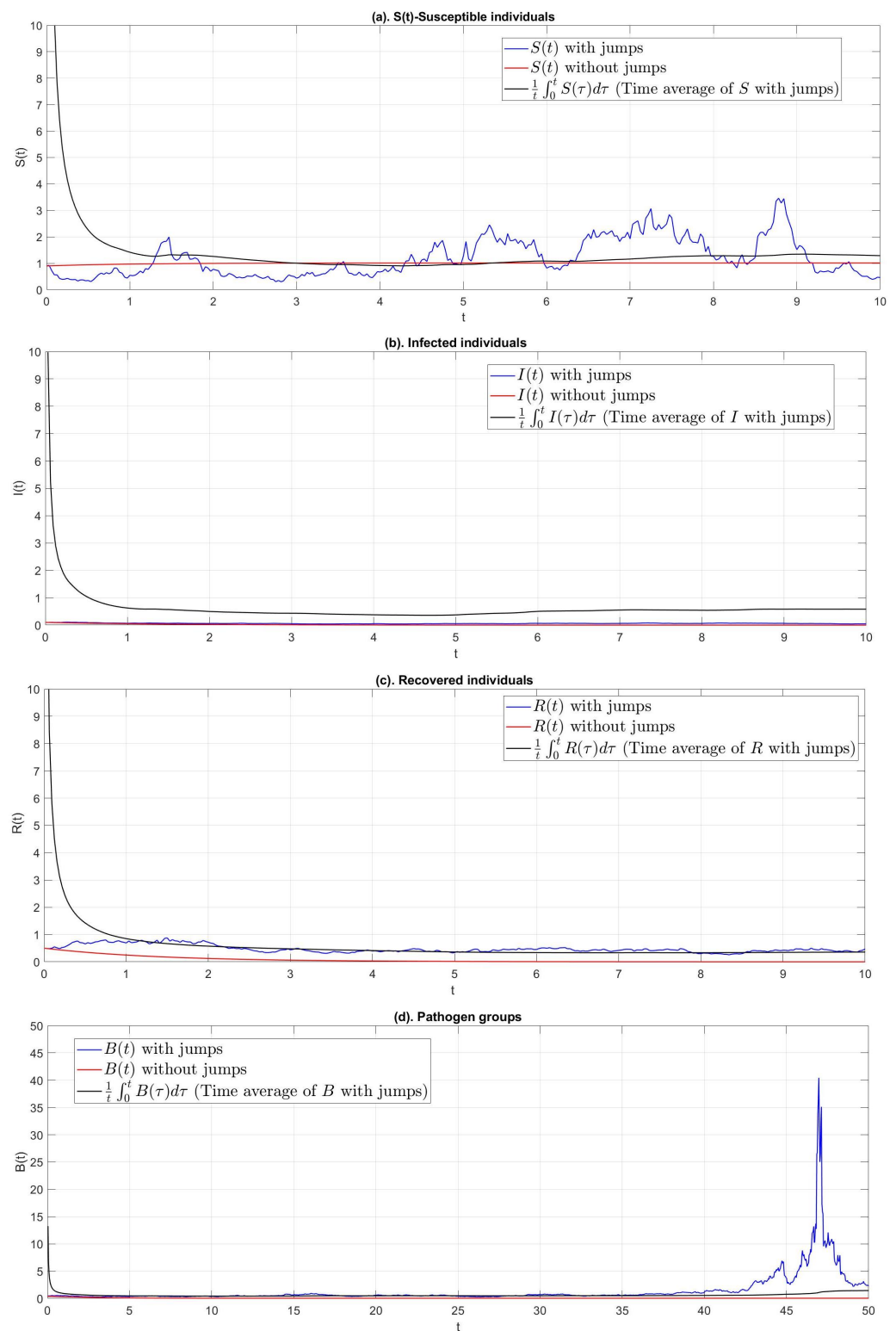### 7.1. Numerical Simulations for Extinction

The initial conditions used for the simulations of the parameters and noise intensities are taken from Table 1 and $\mathcal{Z}_i(x) = \frac{-k_i\mathcal{Z}(x)}{1 + \mathcal{Z}(x)^2}$. In Figure 3, the deterministic system (1) and the perturbed system (3) are simulated and shown concerning the corresponding stochastic threshold value, which meet $\mathbb{R}^s < 1$. These graphs show the trajectory of the type of an exponential function with probability one ensuring that the size of cholera

virus go to zero as time evolves. Theorem 2 is mathematically validated by this finding. Furthermore, it appears from the data that the deterministic and stochastic systems agree closely. Furthermore, the systems' paths eventually converge to the corresponding DFE of the deterministic system.

(a) The blue line depicts the susceptible population's response to disease exposure in the stochastic model, characterized by Lévy jumps that induce immediate declines in susceptibility, while the red line shows the deterministic model's uniform reduction without such perturbations. (b) The infected individual count fluctuates in the stochastic model, marked by intermittent, sharp increases that reflect outbreak events, contrasting with the deterministic model's smooth progression of infection rates. (c) Recovery rates, depicted by the blue line for the stochastic model, exhibit variability reflecting changing conditions, as opposed to the deterministic model's consistent recovery trajectory. (d) Pathogen population levels experience pronounced spikes in the stochastic model, suggesting rapid proliferation phases, while the deterministic model reveals a steady increase and decrease in pathogen levels.

Table 1. Initial conditions and parameters values of the system (1).

Parameter/Initial Condition	Value
ζ	3.50
μ	0.03
β_1	0.05
β_2	0.06
γ	0.03
η	0.02
δ	0.01
δ_1	0.15
δ_2	0.20
δ_3	0.40
δ_4	0.35
$S(0)$	0.90
$I(0)$	0.30
$R(0)$	0.50
$B(0)$	0.40
x	0.60
k_1	0.50
k_2	0.50
k_3	0.30
k_4	0.30
k_5	0.10

Figure 3. Examples of simulations involving the stochastic model (3) and the deterministic model (1) when $\mathbb{R}^s < 1$.
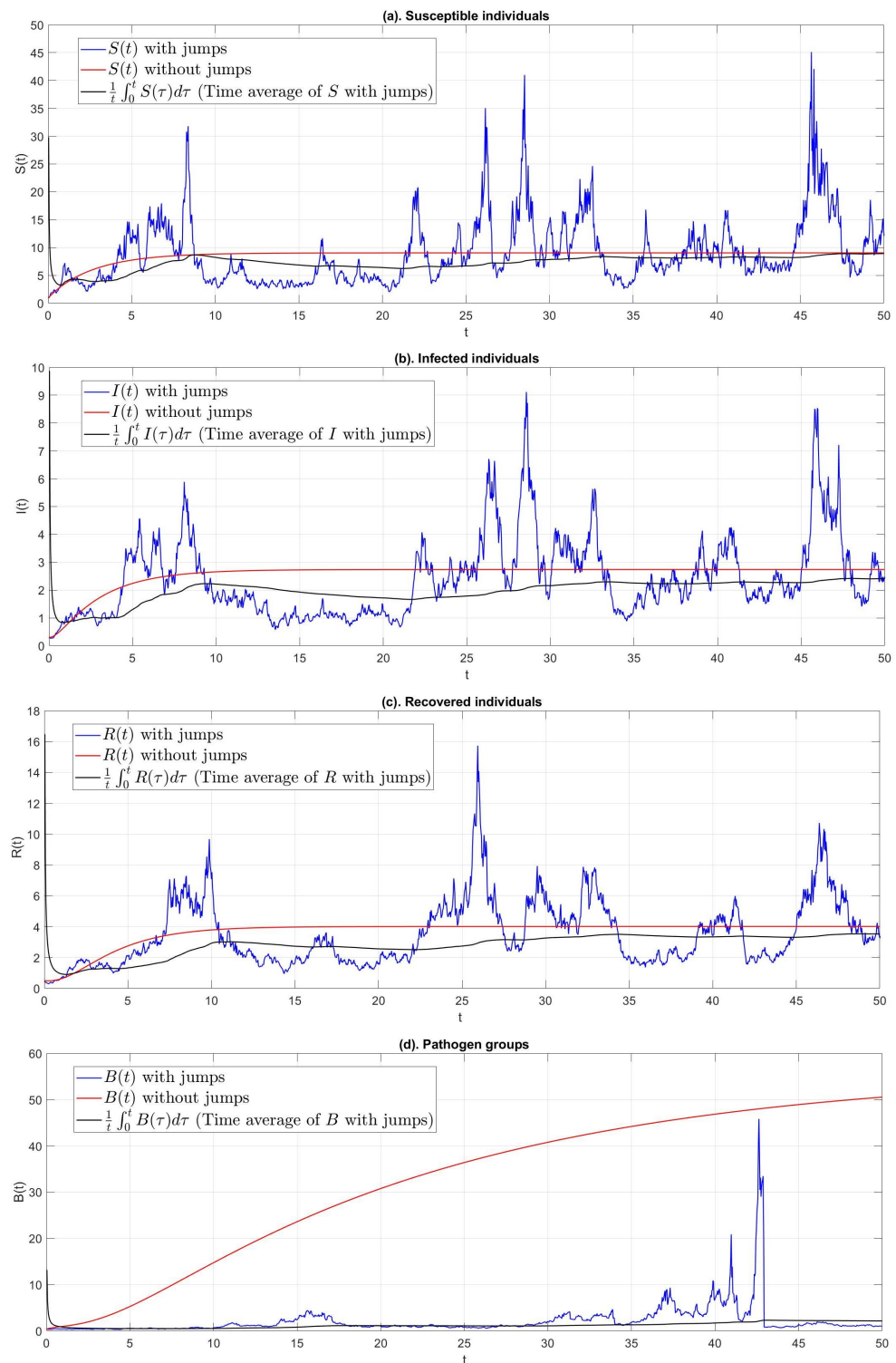
7.2. Numerical Simulations for Persistence

From a biological perspective, we can say that Theorem 3 ensures the persistence of the infection whose dynamics are guaranteed by model (3). We considered another set of parameters and noise intensity values which were taken from Table 2. By closely monitoring the simulations, we can argue that the disease is still spreading among individuals, particularly in environments with low levels of white noise. The non-zero trajectories of the bacteria concentration $\mathcal{B}$ in Figure 4 support this finding and show that there are bacterial concentrations present. This result is consistent with the claim in Theorem 3. Upon closer inspection, the solution behavior of the perturbed model shows that the curves fluctuate around the equilibrium (EE) point of the equivalent deterministic model (1). The results for both systems under the condition of $\mathbb{R}_0^s > 1$ are shown in Figure 4. At each time t, the bacterial concentrations, $\mathcal{B}$, is consistently non-zero. The importance of Theorem 3 for the deterministic model (1) is shown by this result. In particular, when the value of model (3) $\mathbb{R}_0^s$ exceeds unity, the corresponding solution exhibits oscillations around the endemic equilibrium. To effectively control the spread of different bacterial strains and the related population densities in such situations, strong policies that impose strict control measures against different variants are necessary.

This figure compares stochastic (with Lévy jumps) and deterministic models in disease dynamics, emphasizing Lévy noise's utility in modeling sudden, significant changes. (a) Susceptible dynamics show stochastic volatility versus deterministic gradual decline. (b) Infected counts spike in stochastic simulations, underscoring potential outbreaks, unlike the deterministic smooth increase. (c) Recovery rates in the stochastic model vary sharply, contrasting with the deterministic consistency. (d) A late surge in pathogen levels in the stochastic model highlights its capacity to capture critical, abrupt events, advocating for Lévy noise over Gaussian in systems experiencing impactful, discrete changes.

Table 2. Second set of parameters and Initial conditions for the (1).

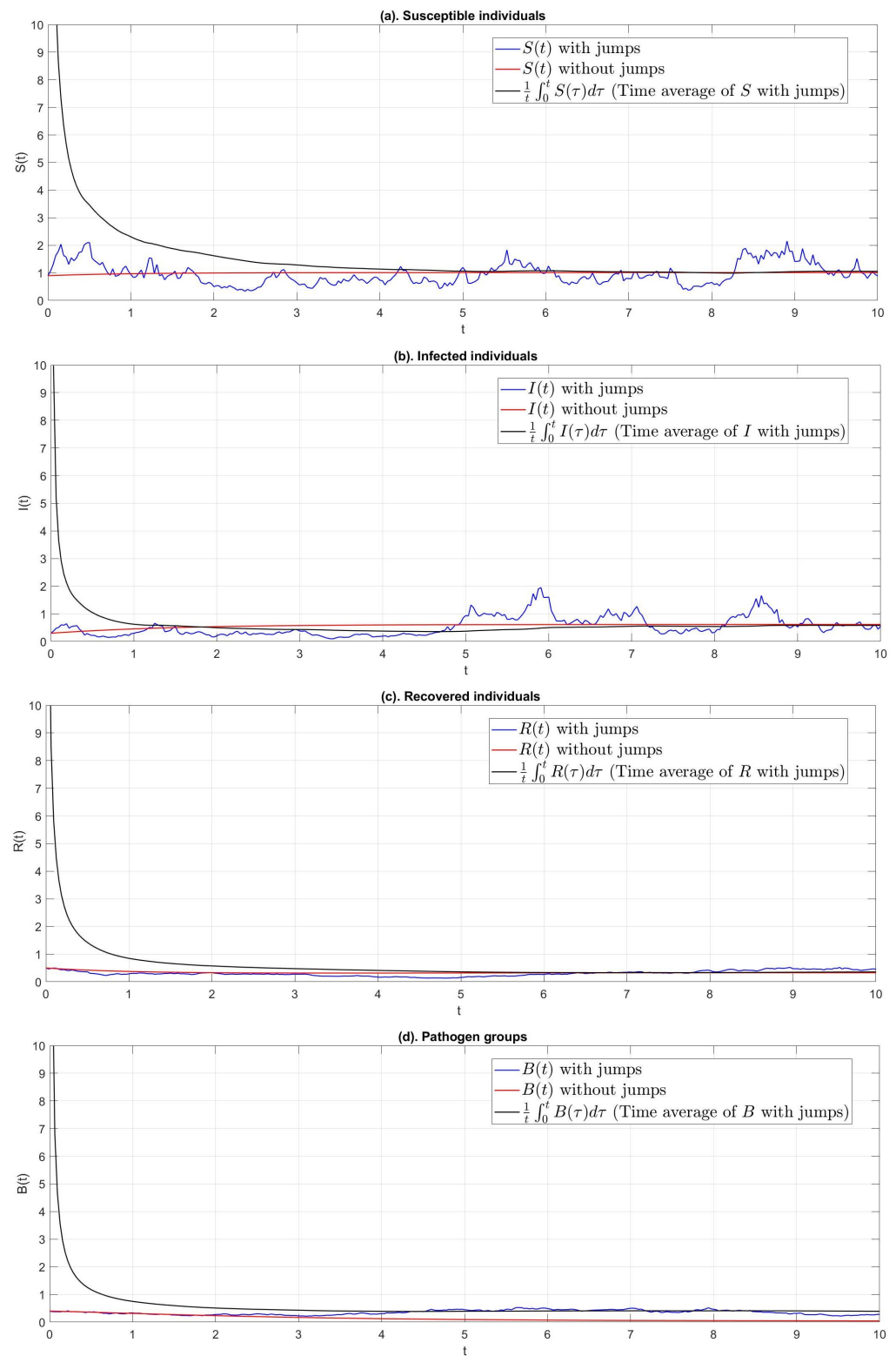| Parameter/Initial Condition	Value
ζ	1.40
μ	0.35
β_1	0.04
β_2	0.05
γ	0.2
η	0.02
δ	0.01
δ_1	0.15
δ_2	0.20
δ_3	0.40
δ_4	0.35
$S(0)$	0.90
$I(0)$	0.30
$R(0)$	0.50
$B(0)$	0.40
x	0.70
k_1	0.50
k_2	0.50
k_3	0.30
k_4	0.20
k_5	0.20

Figure 4. The plot shows the solutions profile obtained through simulations for various compartments of systems (1) and (3).

7.3. Effects of the Noise on Systems (1)

To show the effects of noise then we assumed parameters and noise intensities values $\xi = 1.40$, $\mu = 0.03$, $\beta_1 = 0.04$, $\beta_2 = 0.05$, $\gamma = 0.2$, $\eta = 0.02$, $\delta = 0.01$, $\delta_1 = 0.10$, $\delta_2 = 0.15$, $\delta_3 = 0.20$, $\delta_4 = 0.25$, $\mathcal{S}(0) = 0.90$, $\mathcal{I}(0) = 0.30$, $\mathcal{R}(0) = 0.50$, $\mathcal{B}(0) = 0.40$, and $\mathcal{Z}_i(x) = \frac{-k_i \mathcal{Z}(x)}{1 + \mathcal{Z}(x)^2}$, $x = 0.70$, with $k_1 = 0.50$, $k_2 = 0.50$, $k_3 = 0.30$, $k_4 = 0.20$, $k_5 = 0.20$. Based on observations, it appears that the disease will continue to spread across the population,

especially in areas with low white noise levels. This is consistent with the claim made in Theorem 3. Furthermore, it is clear by analyzing the behaviour of solution to the stochastic system that the curves fluctuate about the endemic fixed point of the equivalent deterministic model (1). Under the condition $\mathbb{R}_0^s > 1$, the solutions for both the systems are graphically shown in Figure 5.

Figure 5. Sample solutions for different classes of the deterministic model (1) and the stochastic model (3).

7.4. Parameter β_1 Impact on $\mathcal{I}(t)$

To investigate the impact of the parameter β_1, we set initial conditions of the system (3) as $\mathcal{S}(0) = 0.90$, $\mathcal{I}(0) = 0.30$, $\mathcal{R}(0) = 0.50$, $\mathcal{B}(0) = 0.40$, and the parameters are $\xi = 1.40$, $\mu = 0.35$, $\beta_2 = 0.5$, $\gamma = 0.2$, $\eta = 0.02$, $\delta = 0.01$, and the noise intensity are $\delta_1 = 0.10$, $\delta_2 = 0.20$, $\delta_3 = 0.40$, $\delta_4 = 0.35$, and $\mathcal{Z}_i(x) = \frac{-k_i \mathcal{Z}(x)}{1+\mathcal{Z}(x)^2}$, $x = 0.70$, with $k_1 = 0.50$, $k_2 = 0.50$, $k_3 = 0.30$, $k_4 = 0.20$, $k_5 = 0.20$. It can be seen in Figure 6, that the fluctuation of the value of the spreader $\mathcal{I}$ becomes larger if increase the value of β_1. The graphical findings in Figure 6a–c demonstrate the biological importance of β_1 parameters. The course of the disease $\mathcal{I}(t)$ in the SDE model is shown by the blue curve, whereas the comparable deterministic model's route of the disease $\mathcal{I}(t)$ is represented by the red curve.

As β_1 increases from 0.10 in Figure 6a to 0.50 in Figure 6c, the stochastic model shows more frequent and severe infection spikes, indicating heightened outbreak risks with greater interaction. In contrast, the deterministic model remains largely unchanged, emphasizing the stochastic model's ability to capture sudden, significant epidemiological events that deterministic models might miss.
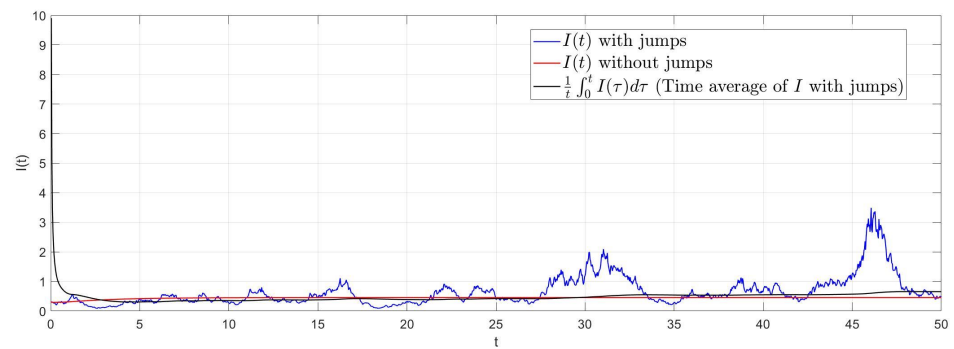
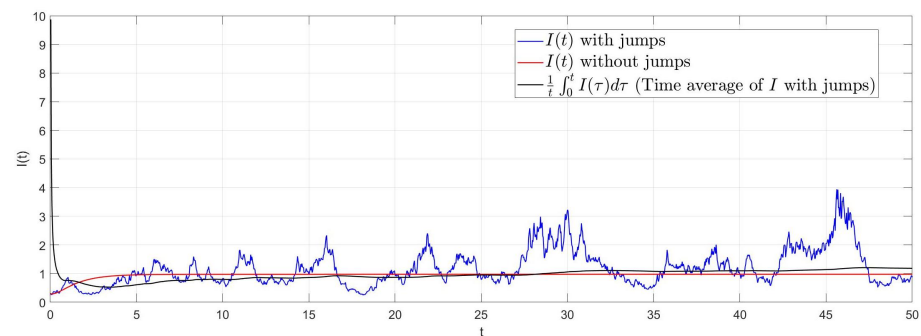(**a**) When $\beta_1 = 0.10$
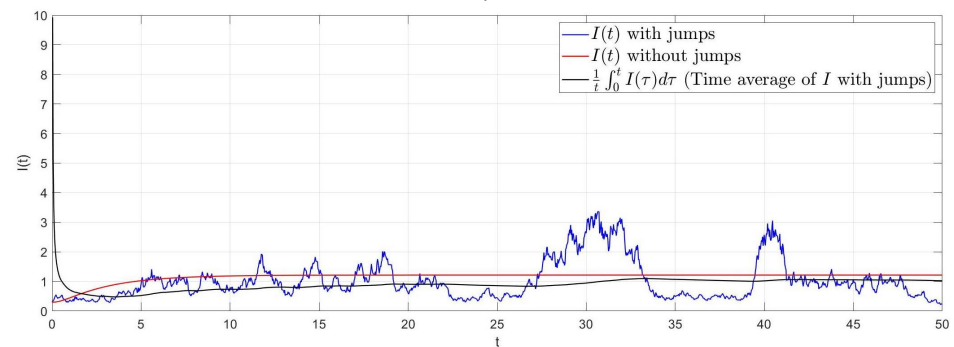
(**b**) When $\beta_1 = 0.30$
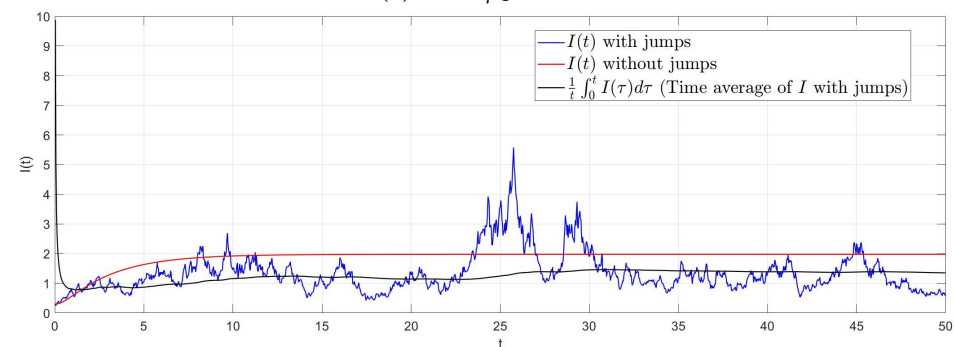
(**c**) When $\beta_1 = 0.50$

Figure 6. The path of $\mathcal{I}(t)$ for the stochastic model (3) and its corresponding deterministic model. This Figure depicts the effect of β_1, the interaction rate between humans and the environment, on infection dynamics in stochastic (blue line) and deterministic (red line) models.
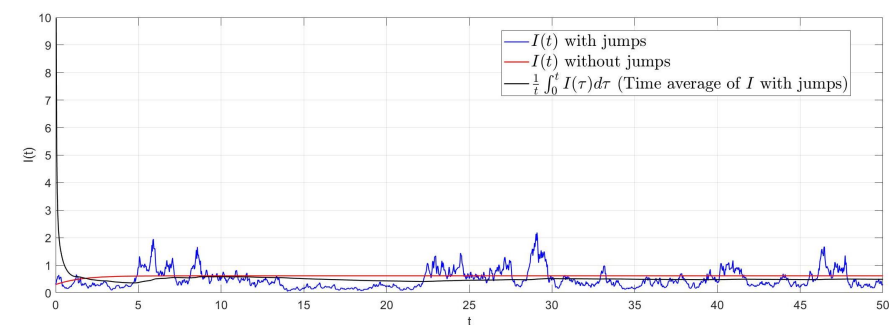
7.5. Parameter β_2 impact on $\mathcal{I}(t)$

To investigate the impact of the parameter β_1, we set initial conditions of the system (3) as $\mathcal{S}(0) = 0.90$, $\mathcal{I}(0) = 0.30$, $\mathcal{R}(0) = 0.50$, $\mathcal{B}(0) = 0.40$, and the parameters are $\xi = 1.40$, $\mu = 0.35$, $\beta_1 = 0.2$, $\gamma = 0.2$, $\eta = 0.02$, $\delta = 0.01$ and the noise intensity are $\delta_2 = 0.20$, $\delta_3 = 0.40$, $\delta_4 = 0.35$, and $\mathcal{Z}_i(x) = \frac{-k_i \mathcal{Z}(x)}{1 + \mathcal{Z}(x)^2}$, $x = 0.70$, with $k_1 = 0.50$, $k_2 = 0.50$, $k_3 = 0.30$, $k_4 = 0.20$, $k_5 = 0.20$. It can be seen in Figure 7, that the fluctuation of the value of the spreader $\mathcal{I}$ becomes larger if increase the value of β_2. The graphical findings in Figure 7a–c demonstrate the biological importance of β_2 parameters. The disease $\mathcal{I}(t)$ of the SDE model is shown by the blue curve, and the disease $\mathcal{I}(t)$ of the matching deterministic model is represented by the red curve.

Figure 7a–c demonstrate varying β_2 levels: 0.20, 0.50, and 0.60, respectively. Increased β_2 correlates with more pronounced and erratic infection spikes in the stochastic model, highlighting the sensitivity to human interaction levels in predicting outbreak patterns. Conversely, the deterministic model shows only minor variations with increasing β_2, underscoring its limitations in capturing the complexity of real-world social interactions and their impacts on disease spread.

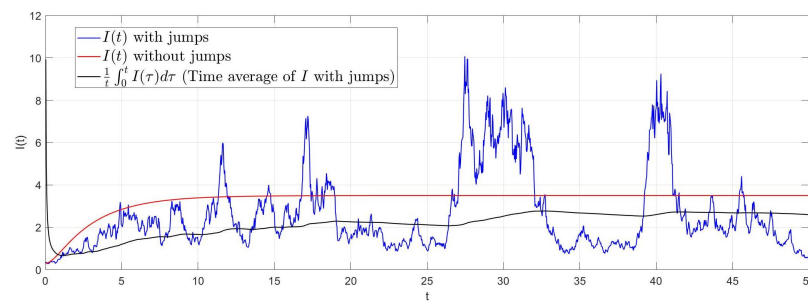(**a**) When $\beta_2 = 0.20$

(**b**) When $\beta_2 = 0.50$
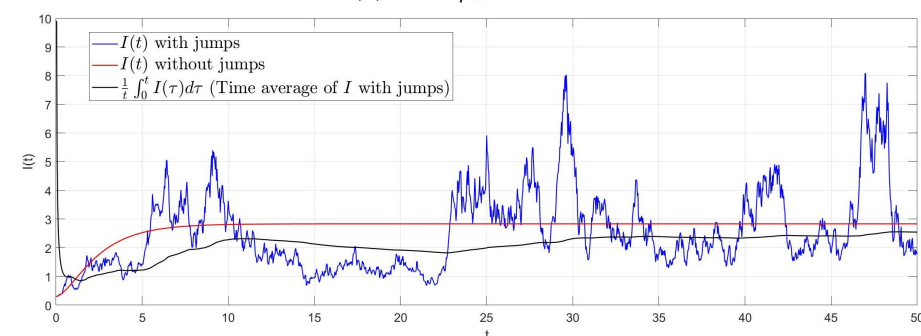
(**c**) When $\beta_2 = 0.60$

Figure 7. The path of $\mathcal{I}(t)$ for the stochastic model (3) and its corresponding deterministic model. This figure explores the impact of β_2, representing human-to-human interaction, on infection dynamics within stochastic (blue line) and deterministic (red line) models.
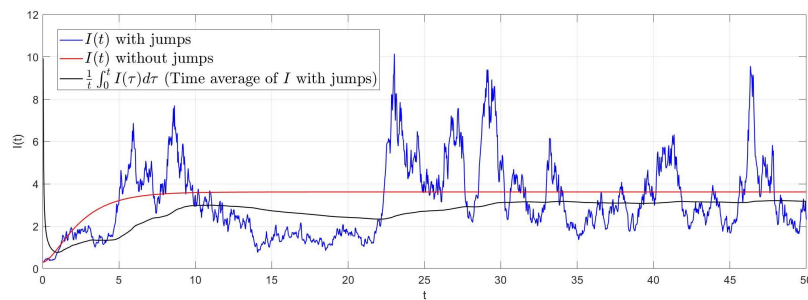
7.6. Noise Intensity Impact on $\mathcal{I}(t)$

To investigate the impact of the parameter β_1, we set initial conditions of the system (3) as $\mathcal{S}(0) = 0.90$, $\mathcal{I}(0) = 0.30$, $\mathcal{R}(0) = 0.50$, $\mathcal{B}(0) = 0.40$, and the parameters are $\xi = 1.40$, $\mu = 0.03$, $\beta_2 = 0.5$, $\gamma = 0.2$, $\eta = 0.02$, $\delta = 0.01$, and $\mathcal{Z}_i(x) = \frac{-k_i \mathcal{Z}(x)}{1 + \mathcal{Z}(x)^2}$, $x = 0.70$, with $k_1 = 0.50$, $k_2 = 0.50$, $k_3 = 0.30$, $k_4 = 0.20$, $k_5 = 0.20$. It can be seen in Figure 8 that the fluctuation of the value of the spreader $\mathcal{I}$ becomes larger if the increase in the value of noise intensity are δ_1, δ_2, δ_3, δ_4. The graphical findings in Figure 8a–c demonstrate the biological importance of δ_1, δ_2, δ_3, δ_4. The disease $\mathcal{I}(t)$ in the Stochastic Differential Equation (SDE) model is represented by the blue curve, and the disease $\mathcal{I}(t)$ in the comparable deterministic model is represented by the red curve. Because of this, lower noise levels contribute to the disease's distinct presence and duration. On the other hand, higher white noise values could cause disease extinction.

The progression from Figure 8a ($\delta_1 = 0.50$, $\delta_2 = 0.35$, $\delta_3 = 0.10$, $\delta_4 = 0.15$) through Figure 8c ($\delta_1 = 0.90$, $\delta_2 = 0.70$, $\delta_3 = 0.50$, $\delta_4 = 0.55$) illustrates an increase in the frequency and amplitude of infection spikes as noise intensities rise. This underscores the importance of Lévy noise in capturing the unpredictable and significant fluctuations typical of epidemic outbreaks, which are not evident in the smoother curves of the deterministic model. The stochastic model, with its ability to simulate these complex dynamics, highlights the critical role of modeling realistic interaction and noise impacts in disease spread predictions.

(a) When $\delta_1 = 0.50$, $\delta_2 = 0.35$, $\delta_3 = 0.10$, $\delta_4 = 0.15$

(b) When $\delta_1 = 0.60$, $\delta_2 = 0.30$, $\delta_3 = 0.50$, $\delta_4 = 0.25$
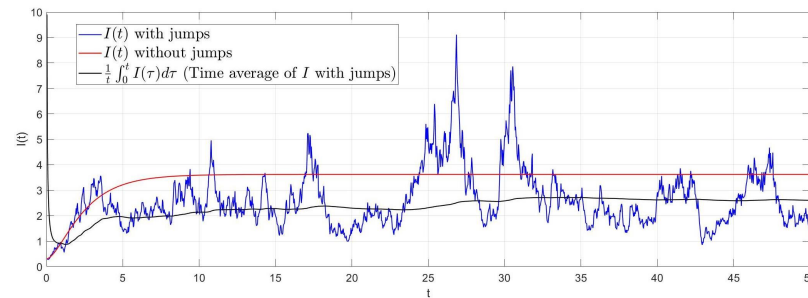

(c) When $\delta_1 = 0.90$, $\delta_2 = 0.70$, $\delta_3 = 0.50$, $\delta_4 = 0.55$

Figure 8. The path of $\mathcal{I}(t)$ for the stochastic model (3) and its corresponding deterministic model. This figure shows the impact of varying noise intensity parameters ($\delta_1, \delta_2, \delta_3, \delta_4$) on infection dynamics in stochastic (blue line) and deterministic (red line) models.

7.7. Comparison of Noises

Figure 9 highlights how Lévy noise can introduce significant variability and extreme events, capturing the unpredictable nature of epidemic outbreaks. The parameters for noise intensity $(\delta_1, \delta_2, \delta_3, \delta_4)$ vary from (0.50, 0.35, 0.10, 0.15) in Gaussian noise to (0.90, 0.70, 0.50, 0.55) in Lévy noise, illustrating the increased amplitude and frequency of infection spikes as noise intensities rise. These effects underscore the critical role of realistic stochastic modeling in capturing the complexities of disease spread. Figure 9a illustrates the effect of Gaussian noise, showing a smooth progression of the susceptible $(S(t))$, infected $(I(t))$, and recovered $(R(t))$ populations, along with the pathogen load $(B(t))$. In contrast, Figure 9b depicts the impact of Lévy noise, demonstrating more pronounced fluctuations and spikes in population dynamics, particularly in the infected population.

(**a**) Gaussian Noise (**b**) Lévy Noise
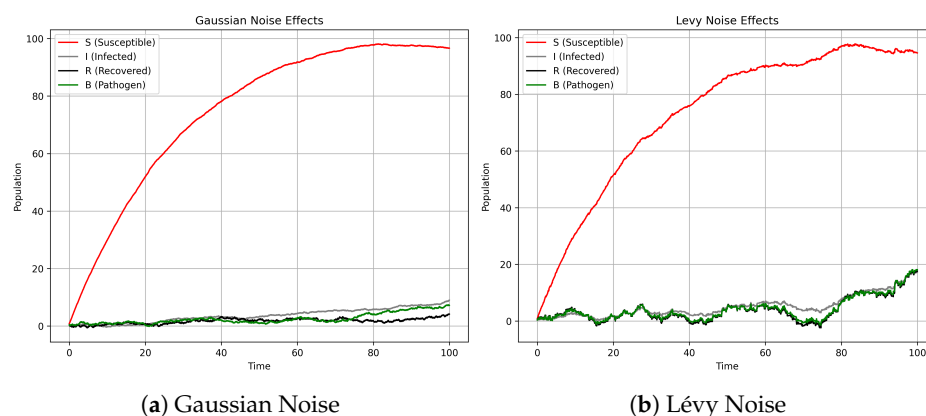
Figure 9. Comparative analysis of infection dynamics under different noise models in a stochastic simulation of an epidemic.

8. Discussion and Conclusions

This work is focused on the understanding of diarrhea transmission in the spread of infectious diseases. We obtained a system of stochastic differential equations from the initially developed deterministic system while considering the effectiveness of Lévy noise in modeling epidemics. Together with stability theorems, the equilibria of the related deterministic model were also formulated. According to our findings, the suggested stochastic model has a single global solution. By using the Lyapunov function theory, we have shown that the system is mean stable when $\mathbb{R}_0^s > 1$. On the other hand, our findings imply that the illness could be effectively eliminated from the population at $\mathbb{R}^s < 1$. We provide graphical solutions to strengthen the validity of our analytical results. Our study delved into understanding how cholera transmission behaves in the long term using mathematical analysis.

Our research demonstrates the unique global solution and mean stability under stochastic influences, a key finding that enhances our understanding of cholera dynamics under random perturbations. In a similar research, [42] investigated the stochastic resonance in a FitzHugh–Nagumo model with additive Lévy noise. They found that Lévy noise induced stochastic resonance phenomena that were different and potentially more advantageous than those induced by Gaussian noise. Furthermore, [43] provided insights into the stochastic stability of cholera models, reinforcing our findings about the model's behavior under different stochastic conditions and adding credibility to our theoretical approach.

Below is Table 3, which lists research papers that argue the advantages of Lévy noise over Gaussian noise in various models. Each entry includes the primary focus of the study, and key results that highlight the benefits of using Lévy noise. These papers collectively suggest that Lévy noise, due to its ability to model jumps and heavy tails, offers significant advantages over Gaussian noise for systems experiencing sudden, significant changes or systems with outliers.

Table 3. Summary of research on noise models and their applications.

Citation	Field	Noise Type	Findings	Distinctive Points
[44]	Subsurface hydrology	Both Lévy and Gaussian	Highlighted advantages of fractional Lévy motion	Extended fractional Gaussian noise to 3D fractals
[45]	Prognostics	Gaussian	Discussed Gaussian noise limitations	Emphasized Lévy noise for large noise levels
[46]	SDEs	Both Lévy and Gaussian	Reviewed advantages of non-Gaussian noises	Illustrated Gaussian noise limitations in SDEs
[47]	Image processing	Non-Gaussian	Explored superiority of non-Gaussian models	Highlighted robustness of Lévy noise in dense matching
[48]	Financial time series	Lévy	Explored Lévy processes' suitability	Compared Lévy and Gaussian processes

Knowing how disease spreads through food and water may be very helpful in reducing the danger of cross-contamination, which differs from conventional person-to-person cholera transmission [49–52]. The three mechanisms of transmission, foodborne, waterborne, and human-to-human, must be addressed to successfully lower the total risk, according to the researchers. The authors hope to expand on this work by including variables linked to disease, age, and regional impacts in future research.

9. Future Recommendations

In the future, we recommend extending the scope of our cholera model to include additional factors that can significantly influence disease dynamics. One such advancement would be the integration of spatial and demographic variables, considering the diverse impact of cholera across different regions and age groups. This would enable a more tailored approach towards predicting and managing outbreaks in specific communities. Another important area is the exploration of varying behavioral responses within populations, especially in reaction to public health interventions, which could lead to more dynamic and adaptive models. The exploration of other forms of stochastic disturbances, beyond Lévy noise, may provide deeper insights into the unpredictability of epidemic patterns. In the realm of computational analysis, the development of more sophisticated numerical methods for solving complex stochastic differential equations could further enhance the accuracy and efficiency of simulations. Collaborations with public health authorities for real-world data acquisition and model validation could significantly improve the practical applicability of our theoretical findings, leading to more effective disease control strategies.

Author Contributions: Conceptualization, Q.T.A.; methodology, A.D.; software, A.D.; validation X.Q. and Z.K.; formal analysis, Q.T.A.; investigation, A.D.; resources, X.Q. and Z.K.; data curation, Q.T.A. and A.D.; writing—original draft preparation, Q.T.A.; writing—review and editing, A.D., X.Q. and Z.K.; visualization, Q.T.A.; supervision, X.Q. and Z.K.; project administration, X.Q. and Z.K.; funding acquisition, X.Q. and Z.K. All authors have read and agreed to the published version of the manuscript.

Data Availability Statement: Data are contained within the article.

Conflicts of Interest: The authors declare no conflicts of interest.

References

1. Cui, J.; Wu, Z.; Zhou, X. Mathematical analysis of a cholera model with vaccination. *J. Appl. Math.* **2014**, *2014*, 324767. [CrossRef]
2. Kirschner, A.K.T.; Schlesinger, J.; Farnleitner, A.H.; Hornek, R.; SüB, B.; Golda, B.; Herzig, A.; Reitner, B. Rapid growth of planktonic vibrio cholerae non-O1/non-O139 strains in a large alkaline lake in Austria: Dependence on temperature and dissolved organic carbon quality. *Appl. Environ. Microbiol.* **2008**, *74*, 2004–2015. [CrossRef] [PubMed]

3. Reidl, J.; Klose, K.E. Vibrio cholerae and cholera: Out of the water and into the host. *FEMS Microbiol. Rev.* **2002**, *26*, 125–139. [CrossRef] [PubMed]

4. Shuai, Z.; Tien, J.H.; Driessche, P.V.D. Cholera models with hyperinfectivity and temporary immunity. *Bull. Math. Biol.* **2012**, *74*, 2423–2445. [CrossRef] [PubMed]

5. Centers for Disease Control and Prevention. Cholera Vibrio Cholerae Infection. 2018. Available online: https://www.cdc.gov/cholera/general/index.html (accessed on 15 January 2024).

6. Mwasa, A.; Tchuenche, J.M. Mathematical analysis of a cholera model with public health interventions. *Biosystems* **2011**, *105*, 190–200. [CrossRef] [PubMed]

7. Neilan, R.L.M.; Schaefer, E.; Gaff, H.; Fister, K.R.; Lenhart, S. Modeling optimal intervention strategies for cholera. *Bull. Math. Biol.* **2010**, *72*, 2004–2018.

8. Beryl, M.O.; George, L.O.; Fredrick, N.O. Mathematical analysis of a cholera transmission model incorporating media coverage. *Int. J. Pure Appl. Math.* **2016**, *111*, 219–231. [CrossRef]

9. Sun, G.Q.; Xie, J.H.; Huang, S.H.; Jin, Z.; Li, M.T.; Liu, L. Transmission dynamics of cholera: Mathematical modeling and control strategies. *Commun. Nonlinear Sci.* **2017**, *45*, 235–244. [CrossRef]

10. Wang, J.; Modnak, C. Modeling cholera dynamics with controls. *Can. Appl. Math. Q.* **2011**, *19*, 255–273.

11. Meetei, M.Z.; Zafar, S.; Zaagan, A.A.; Mahnashi, A.M.; Idrees, M. Dengue Transmission Dynamics: A Fractional-Order Approach with Compartmental Modeling. *Fractal Fract.* **2024**, *8*, 207. [CrossRef]

12. De la Sen, M.; Ibeas, A.; Alonso-Quesada, S.; Nistal, R. On a new epidemic model with asymptomatic and dead-infective subpopulations with feedback controls useful for Ebola disease. *Discrete Dyn. Nat. Soc.* **2017**, *2017*, 4232971. [CrossRef]

13. Wajaree, W.; Botmart, T.; La-inchua, T.; Sabir, Z.; Núñez, R.A.S.; Abukhaled, M.; Guirao, J.L.G. A stochastic computational scheme for the computer epidemic virus with delay effects. *AIMS Math.* **2023**, *8*, 148–163.

14. Sabbar, Y.; Din, A.; Kiouach, D. Influence of fractal-fractional differentiation and independent quadratic Lévy jumps on the dynamics of a general epidemic model with vaccination strategy. *Chaos Soliton. Fract.* **2023**, *171*, 113434. [CrossRef]

15. Zhang, Y.H.; Ma, X.; Din, A. Stationary distribution and extinction of a stochastic SEIQ epidemic model with a general incidence function and temporary immunity. *AIMS Math.* **2021**, *6*, 12359–12378. [CrossRef]

16. Lin, S.; Zhang, J.; Qiu, C. Asymptotic Analysis for One-Stage Stochastic Linear Complementarity Problems and Applications. *Mathematics* **2023**, *11*, 482. [CrossRef]

17. Wang, Y.; Xu, J.; Qiao, L.; Zhang, Y.; Bai, J. Improved amplification factor transport transition model for transonic boundary layers. *AIAA J.* **2023**, *61*, 3866–3882. [CrossRef]

18. Hu, J.; Wu, Y.; Li, T.; Ghosh, B.K. Consensus control of general linear multiagent systems with antagonistic interactions and communication noises. *IEEE Trans. Autom. Control* **2018**, *64*, 2122–2127. [CrossRef]

19. Lemos-Paião, A.P.; Maurer, H.; Silva, C.J.; Torres, D.F.M. A SIQRB delayed model for cholera and optimal control treatment. *Math. Model. Nat. Phenom.* **2022**, *17*, 25. [CrossRef]

20. Li, D.; Wei, F.; Mao, X. Stationary distribution and density function of a stochastic SVIR epidemic model. *J. Frankl. I.* **2022**, *359*, 9422–9449. [CrossRef]

21. Liu, Q.; Jiang, D.; Hayat, T.; Alsaedi, A. Dynamical behavior of a stochastic epidemic model for cholera. *J. Frankl. I.* **2019**, *356*, 7486–7514. [CrossRef]

22. Wei, F.; Jiang, H.; Zhu, Q. Dynamical behaviors of a heroin population model with standard incidence rates between distinct patches. *J. Frankl. I.* **2021**, *358*, 4994–5013. [CrossRef]

23. Danane, J.; Yavuz, M.; Yıldız, M. Stochastic modeling of three-species Prey–Predator model driven by Lévy Jump with Mixed Holling-II and Beddington–DeAngelis functional responses. *Fractal Fract.* **2023**, *7*, 751. [CrossRef]

24. Huo, L.A.; Dong, Y.F.; Lin, T.T. Dynamics of a stochastic rumor propagation model incorporating media coverage and driven by Lévy noise. *Chin. Phys. B* **2021**, *30*, 080201. [CrossRef]

25. De la Sen, M.; Alonso-Quesada, S.; Ibeas, A. On the stability of an SEIR epidemic model with distributed time-delay and a general class of feedback vaccination rules. *Appl. Math. Comput.* **2015**, *270*, 953–976. [CrossRef]

26. Xie, Y.; Liu, Z. The unique ergodic stationary distribution of two stochastic SEIVS epidemic models with higher order perturbation. *Math. Biosci. Eng.* **2023**, *20*, 1317–1343. [CrossRef] [PubMed]

27. Applebaum, D. *Lévy Processes and Stochastic Calculus*; Cambridge University Press: Cambridge, UK, 2009.

28. Li, S. SIR Epidemic Model with General Nonlinear Incidence Rate and Lévy Jumps. *Mathematics* **2024**, *12*, 215. [CrossRef]

29. Kiouach, D.; Azami El-idrissi, S.E.; Sabbar, Y. The impact of Lévy noise on the threshold dynamics of a stochastic susceptible-vaccinated-infected-recovered epidemic model with general incidence functions. *Math. Methods Appl. Sci.* **2024**, *47*, 297–317. [CrossRef]

30. Chen, C.; Kang, Y. Dynamics of a stochastic multi-strain SIS epidemic model driven by Lévy noise. *Commun. Nonlinear Sci. Numer. Simul.* **2017**, *42*, 379–395. [CrossRef]

31. Boukanjime, B.; El Fatini, M. A stochastic Hepatitis B epidemic model driven by Lévy noise. *Phys. A Stat. Mech. Its Appl.* **2019**, *521*, 796–806. [CrossRef]

32. Yang, H.; Jin, Z. Stochastic SIS epidemic model on network with Lévy noise. *Stoch. Anal. Appl.* **2022**, *40*, 520–538. [CrossRef]

33. Kawamura, A. Lipschitz continuous ordinary differential equations are polynomial-space complete. *Comput. Complex.* **2010**, *19*, 305–332. [CrossRef]

34. Honary, T.G.; Mahyar, H. Approximation in Lipschitz algebras. *Quaest. Math.* **2000**, *23*, 13–19. [CrossRef]

35. Korneichuk, N.P.; Polovina, A.I. Algebraic-polynomial approximation of functions satisfying a Lipschitz condition. *Math. Notes Acad. Sci. USSR* **1971**, *9*, 254–257. [CrossRef]

36. Schlage-Puchta, J.C. Optimal version of the Picard–Lindelöf theorem. *Electron. J. Qual. Theory Differ. Equ.* **2021**, *2021*, 1–8. [CrossRef]

37. El Fatini, M.; Sekkak, I. Lévy noise impact on a stochastic delayed epidemic model with Crowly–Martin incidence and crowding effect. *Phys. A Stat. Mech. Its Appl.* **2020**, *541*, 123315. [CrossRef]

38. Din, A.; Li, Y. Lévy noise impact on a stochastic hepatitis B epidemic model under real statistical data and its fractal–fractional Atangana–Baleanu order model. *Phys. Scr.* **2021**, *96*, 124008. [CrossRef]

39. Skorokhod, A.V. *Asymptotic Methods in the Theory of Stochastic Differential Equations*; American Mathematical Society: Ann Arbor, MI, USA , 2009; Volume 78.

40. Evans, L.C. *An Introduction to Stochastic Differential Equations*; American Mathematical Society: Ann Arbor, MI, USA, 2012; Volume 82.

41. Mao, X. *Stochastic Differential Equations and Applications*; Elsevier: Amsterdam, The Netherlands , 2007.

42. Wang, Z.; Xu, Y.; Yang, H. Lévy noise induced stochastic resonance in an FHN model. *Sci. China Technol. Sci.* **2016**, *59*, 371–375. [CrossRef]

43. Ara, R.; Ahmad, S.; Khan, Z.A.; Zahri, M. Threshold dynamics of stochastic cholera epidemic model with direct transmission. *AIMS Math.* **2023**, *8*, 26863–26881. [CrossRef]

44. Molz, F.J.; Liu, H.H.; Szulga, J. Fractional Brownian motion and fractional Gaussian noise in subsurface hydrology: A review, presentation of fundamental properties, and extensions. *Water Resour. Res.* **1997**, *33*, 2273–2286. [CrossRef]

45. An, D.; Kim, N.H.; Choi, J.-H. Practical options for selecting data-driven or physics-based prognostics algorithms with reviews. *Reliab. Eng. Syst. Saf.* **2015**, *133*, 223–236. [CrossRef]

46. Falsone, G. Stochastic differential calculus for Gaussian and non-Gaussian noises: A critical review. *Comm. Nonlinear Sci.* **2018**, *56*, 198–216. [CrossRef]

47. Deledalle, C.A.; Tupin, F.; Denis, L. Patch similarity under non Gaussian noise. In Proceedings of the 2011 18th IEEE International Conference on Image Processing, Brussels, Belgium, 11–14 September 2011; pp. 1845–1848.

48. Barndorff-Nielsen, O.E.; Mikosch, T.; Resnick, S.I. (Eds.) *Lévy Processes: Theory and Applications*; Springer Science & Business Media: Berlin/Heidelberg, Germany, 2001.

49. Tian, J.P.; Wang, J. Global stability for cholera epidemic models. *Math. Biosci.* **2011**, *232*, 31–41. [CrossRef] [PubMed]

50. Bao, B.; Zhang, Q.M. Stationary distribution and extinction of a stochastic SIRS epidemic model with information intervention. *Adv. Differ. Equ.* **2017**, 1–19.. [CrossRef]

51. Zhang, H.; Xu, Y.; Li, Y.; Kurths, J. Statistical solution to SDEs with α-stable Lévy noise via deep neural network. *Int. J. Dyn. Control* **2020**, *8*, 1129–1140. [CrossRef]

52. Zuo, Z.; Yang, C.; Wang, Y. A new method for stability analysis of recurrent neural networks with interval time-varying delay. *IEEE Trans. Neural Netw.* **2009**, *21*, 339–344.